FINITE-ELEMENT MODEL OF THE HUMAN EARDRUM AND MIDDLE EAR

Sam J. Daniel, Department of Otolaryngology,

McGill University,

Montréal, Québec

July 2002

A thesis submitted to the Faculty of Graduate Studies and Research
in partial fulfilment of the requirements for the degree of

Master of Otolaryngology

Your file Votre référence
ISBN: 0-612-85781-6
Our file Notre référence
ISBN: 0-612-85781-6

Unlike seeing, where one can look away, one cannot 'hear away' but must listen ... hearing implies already belonging together in such a manner that one is claimed by what is being said.

- Hans-Georg Gadamer

Dedication: This thesis is dedicated to my parents. My father Dr S. Abou-Khalil, currently struggling with severe end-stage Parkinson`s disease, has been my role model for compassion, dedication, altruism, and "real" patient care.
Thank you mom for always being there. I would not have gone far in life without your support and love.

ABSTRACT

Computer-generated models are increasingly being used in otolaryngology for teaching purposes, pre-operative planning and clinical simulations, especially when dealing with small complex areas such as the middle ear.

One technique used to analyse the mechanics of complex models is the finite-element method whereby the system of interest is divided into a large number of small simple elements. The mechanical properties and applied forces are represented by functions defined over each element, and the mechanical response of the whole system can then be computed.

A unique three-dimensional finite-element model of the human eardrum and middle ear was devised. This model takes advantage of phase-shift moiré shape measurements to precisely define the shape of the eardrum. The middle-ear geometry is derived from histological serial sections and from high-resolution magnetic-resonance microscopy of the human ear.

The model allows an improved understanding of the mechanics of the human middle ear, can simulate various pathological conditions, and assist in the design of ossicular prostheses.

RÉSUMÉ

Des modèles informatisés sont de plus en plus utilisés en Oto-Rhino-Laryngologie pour des fins educatives, la planification pré-opératoire, et diverse simulations cliniques. Ceci s'avère surtout utile lorsqu'on travaille sur des régions compliquées tel-que l'oreille moyenne.

Une technique utilisée afin d'analyser la mécanique de modèles complexes est la méthode de modèle d'éléments finis où le système d'intérêt est divisé en un grand nombre de petits éléments simples. Les données mécaniques et les forces appliquées sont représentés par des fonctions définies pour chaque élément. Finalement, le comportement mécanique de tout le système est determiné.

Un modèle d'éléments finis tri-dimentionel du tympan et de l'oreille moyenne humaine a été créé. Ce modèle se base sur les mesures précises avec la technique moiré afin d'établir le contour du tympan. La géométrie complexe de l'oreille moyenne a été établie au moyen de coupes histologiques ainsi-que de données de microscopie à résonance magnétique.

Le modèle nous permet de mieux comprendre la mécanique de l'oreille moyenne humaine, de simuler diverses pathologies affectant cette dernière ainsi-que de permettre une meilleure conception de prothèses auditives.

TABLE OF CONTENTS

LIST OF FIGURES AND TABLES

ACKNOWLEDGEMENTS

I would like to take this opportunity to thank humbly all the people who helped me achieve this work. I wish to let them know that they hold a great place in my mind and my heart. In particular, I wish to thank my supervisor, Professor W. Robert J. Funnell, for being a role model, a guide, and a great support; my parents for their endless love and understanding; my colleagues and friends Anthony Zeitouni, Melvin Schloss, Jamie Rappaport, Bernard Segal, René van Wijhe, and Saumil Merchant for their input and support.

This work was supported in part by the Canadian Institutes of Health Research, the Natural Sciences and Engineering Research Council and the department of Otolaryngology of McGill University. I also thank M. M. Henson and O. W. Henson, Jr. (University of North Carolina at Chapel Hill) and The Center for In Vivo Microscopy (Duke University) for providing the MRM data. Special thanks also go to Willem Decraemer (Antwerp University, Belgium) for the moiré data, as well as Clarinda Northrop (Temporal Bone Foundation, Boston) and Shyam Khanna (Columbia University, New York) for the histology datasets.

Chapter 1

INTRODUCTION

1.1 Background

Computer technology has improved dramatically over the past few years, concomitantly with major advances in imaging tools. This has led to revolutionary changes in our medical practice such as pre-surgical and intra-operative 3-dimensional visualization of structures, as well as numerous virtual endoscopic techniques ranging from colonoscopy to bronchoscopy, angiography, and very recently otoscopy (Frankenthaler et al., 1998). There have also been remarkable advances in vibration-measurement technology. In the early years of middle-ear research, scientists like Helmholtz and Politzer had to resort to rudimentary methods such as gluing rods or bird feathers to the ossicles in order to detect vibrations with auditory stimulation of the middle ear (Hüttenbrink, 1995). During these experiments, the sound intensity required to detect the vibrations was very large, resulting in a nonphysiological behaviour of the middle ear. Commercially available laser Doppler vibrometers now permit accurate assessment of middle-ear mechanics with physiological sound pressures. Displacements in the ear down to 10^{-4} microns can easily be measured over a wide range of frequencies, allowing us to validate theoretical models in an experimental setting (Ball et al., 1997).

The combination of the improvements in computers, imaging and measurement technology have made it possible to construct, simulate and validate detailed computer-based models of the ear that previously would not have been feasible.

1.2 Evolution of middle-ear models

1.2.1 Electrical circuit models

Many mathematical models have been constructed over the past few decades, mostly in the form of mechano-acoustical circuits or their equivalent electrical circuits. In these

models the behaviour of the anatomical structure studied is represented by the combination of three kinds of idealized circuit elements: an ideal spring, a point mass, and an ideal damper. An illustration of such a model is presented in Figure 1.1. The parameter values in the model are obtained by trying to match the behaviour of the model with the experimental results. Examples of such models are the ones described by Zwislocki (1962), Shaw & Stinson (1981) and Vlaming (1986). While these so-called "lumped-parameter" techniques can lead to models able to replicate specified experimental data, their biggest disadvantage lies in the fact that their parameters are not closely tied to anatomical or physiological data independently of the behaviour being modelled.

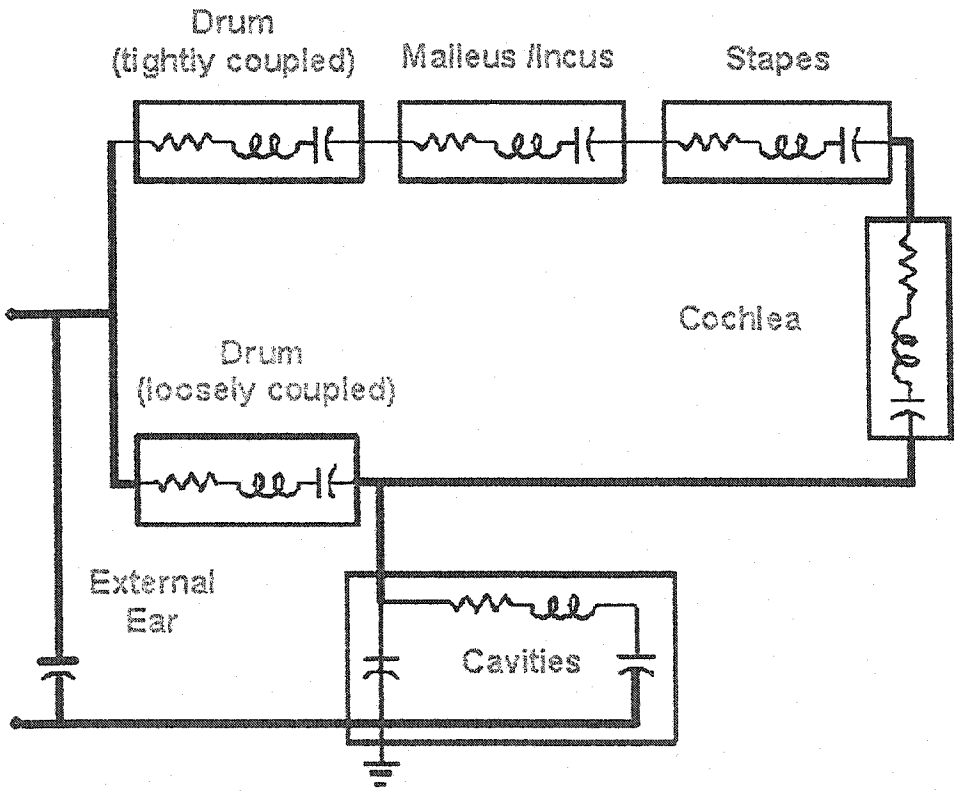

Figure 1.1 Schematic diagram illustrating an example of electrical circuit model.
Adapted from Funnell, 1972.

1.2.2 Recent non-"lumped-parameter" models

More recently, various models that are not of the lumped or circuit type have been devised. An example is the model of Wada & Kobayashi (1990). It consists of a plane-plate distributed representation of the eardrum coupled to a linear lumped model of the normal middle ear in order to simulate tympanometric data; stiffness of the ossicular chain varies as a function of static ear-canal pressure. Another example consists of a representation of eardrum mechanics by using asymptotic techniques to formulate approximate analytical models (Rabbitt & Holmes, 1986; Fay et al., 1999).

While these approaches lead to models that are computationally simpler than a finite-element model, their entire formulations are critically dependent on every assumption and approximation made during the analysis. This makes it much more difficult either to modify assumptions or to refine approximations, and essentially impossible to model the details of realistic geometries.

1.2.3 Finite-element models

The finite-element method is a numerical technique that has found application in many areas. It consists of dividing the system of interest into a number of discrete two- or three-dimensional sub-regions called elements. These elements can have protean shapes such as triangles and quadrilaterals (plates), tetrahedra (pyramids), hexahedra (bricks), etc. The process of dividing a region into elements is known as mesh generation. The mechanical behaviour of each element is then analysed and its response to applied loads is expressed in terms of the displacements of its edges. The geometries of these elements are simple enough to allow analytical intra-element solutions of the differential equations. The result of the relatively simple element analysis is a matrix equation relating the response of the element to the applied forces. The components of these matrix equations are functions of the shapes and material properties of the elements. Finally, all the individual element matrix equations can be combined into a global matrix equation describing the behaviour of the entire complex structure.

The finite-element method has many attractive features. It can easily handle irregular boundary shapes, non-linearities, complex geometries, and inhomogeneities. As a result, the model can accurately represent the anatomy, physiology, and biomechanical properties of the system studied rather than rely on an electrical circuit with variously assigned parameters. The finite-element model has relatively few free parameters whose values need to be adjusted to fit the experimental data. The parameters have a very direct relationship to the structure and function of the system analysed, and can be estimated independently of the particular experimental situation being modelled.

Funnell (1975) was the pioneer in using the finite-element method as a tool for analysing the mechanical behaviour of the middle ear. In fact, the first published finite-element model of the eardrum and middle ear was that of Funnell & Laszlo (1978) for the cat, based on an extensive review of the anatomical, structural and biomechanical nature of the eardrum. Over the past decade it has become clear that the complex geometry and mechanical properties of the middle ear cannot be adequately modelled using circuit models, and the finite-element method has become the technique of choice. Funnell has refined his model over the years as elastic suspensions of the malleus and incus were added, and the mass and damping of the structure was also taken into account (e.g., Funnell et al., 1992).

While Funnell has been, to my knowledge, the first as well as the most persistent and thorough finite-element ear modeller, hearing research seems to have woken up to this technique over the past decade. In fact, effervescence has been observed in middle-ear modelling research, materializing itself not only by the European Colloquium on the "Biomechanics of Hearing" in Stuttgart, Germany [September 1997] but also by the "birth" of international symposia on "middle-ear mechanics in research and otosurgery". The first one was held in Dresden, Germany, in 1996. I was fortunate to attend the second symposium [October 1999] held at the Massachusetts Eye and Ear Infirmary, where I was impressed by the number of engineers, physicists, scientists, and clinicians putting their knowledge towards a better understanding of middle-ear mechanics. This awakening and resurgence of interest in middle-ear modelling is a testimony to an increased awareness in

the scientific community that "our current view of middle-ear function does not explain the hearing losses produced by many middle-ear pathologies" (Rosowski, 1999). This revival is also fuelled by advances in computer technology and the "realization that models can be used to investigate functions of the ear that are not readily observable"(Rosowski, 1999). Table 1 gives a synopsis of existing finite-element models of the **human** outer and middle ear.

Williams & Lesser (1990)	3-D model of TM
Lesser et al (1991)	2-D plain-strain model of the ossicular chain
Wada et al (1992)	3-D middle-ear model
Williams & Lesser (1992)	3-D model of the TM
Koike et al (1996)	3-D middle-ear model including muscles, ligaments & cavity
Beer et al (1997)	3-D model of malleus and TM
Eber (1997)	3-D multibody analysis of the ossicular chain
Zahnert et al (1997)	3-D model with a Dresden PORP prosthesis
Blayney et al (1997)	3-D model of a stapedectomy with damping at the stapes footplate
Drescher J, Schmidt R, Hardtke HJ(1998)	3-D model of TM
Prendergast PJ (1999)	3-D model of middle ear with PORP prosthesis
Ferris P, Prendergast PJ (2000)	3-D model of outer and middle ear with simulations of TORP and PORP ossicular prostheses

Table 1.1 Summary of previous finite-element models of the human middle ear. (TM: tympanic membrane; PORP: partial ossicular replacement prosthesis; TORP: total ossicular replacement prosthesis).

The models outlined in the table above differ significantly from the one that I shall be presenting in this thesis. In fact, the latter is unique in that it uses exact anatomical data derived from moiré shape measurements of the tympanic membrane, histological serial sections, and high-resolution magnetic-resonance images. I feel that designing a realistic anatomical three-dimensional model is of prime importance in order to reduce the number of free parameters in the model. Moiré data provide exact shape measurements for the tympanic membrane, while the histological serial sections and the magnetic-resonance microscopy provide exact data for ossicular, ligamentous and muscular anatomy.

Devising a realistic model allows a better understanding of middle-ear pathology, and bridges a gap between basic science and clinical science in using the former to address the most fundamental clinical issues.

The model will contribute to the understanding of middle-ear mechanics. It also gives more insight into specific clinical pathologies such as ossification of the anterior mallear ligament. It may also contribute to many other clinical applications, such as the design of ossicular prostheses.

Chapter two presents a general overview of the human auditory system with a particular emphasis on the eardrum and middle ear. Chapter three presents the finite-element method; and Chapter four presents the modelling algorithm. Chapter five gives a description of the actual model and the simulation results. The clinical applications and potential future uses of the model are detailed in Chapter six.

Chapter 2

AUDITORY SYTEM

2.1 Overview of the hearing system

Hearing physiology is exquisitely complex and involves multiple steps that interact at various levels, contributing to the hearing process. The human auditory system can be divided into (1) the peripheral sound-conducting apparatus consisting of the external auditory canal, the eardrum, and the middle ear; (2) the auditory component of the inner ear (i.e., the cochlea); and (3) the auditory nervous system consisting of the ascending and descending auditory pathways and the primary and secondary auditory cortical areas.

The external ear aids in sound localisation and delivers sound to the middle ear. Sound is transmitted via the middle-ear ossicles to the oval window. It causes a pressure wave that sets the cochlear fluids into motion. The hair cells present along the basilar membrane sense this motion and their output controls the discharge pattern of the fibres of the auditory nerve. Information is modulated and carried by the ascending auditory pathway to the primary and associative auditory cortical areas.

Of all the parts that are vital for the otolaryngologist to master, the middle ear wins the first vote. This is the most common area of the auditory system wherein surgical treatment can make a difference in correcting a hearing problem, and basic knowledge of middle-ear mechanics is a pre-requisite in obtaining optimal results in reconstructive procedures. To gain a better understanding of the mechanical behaviour and properties of the middle ear, models are developed. Figure 2.1 shows a schematic representation of the peripheral auditory system. In this chapter the focus will be placed on the eardrum and middle ear.

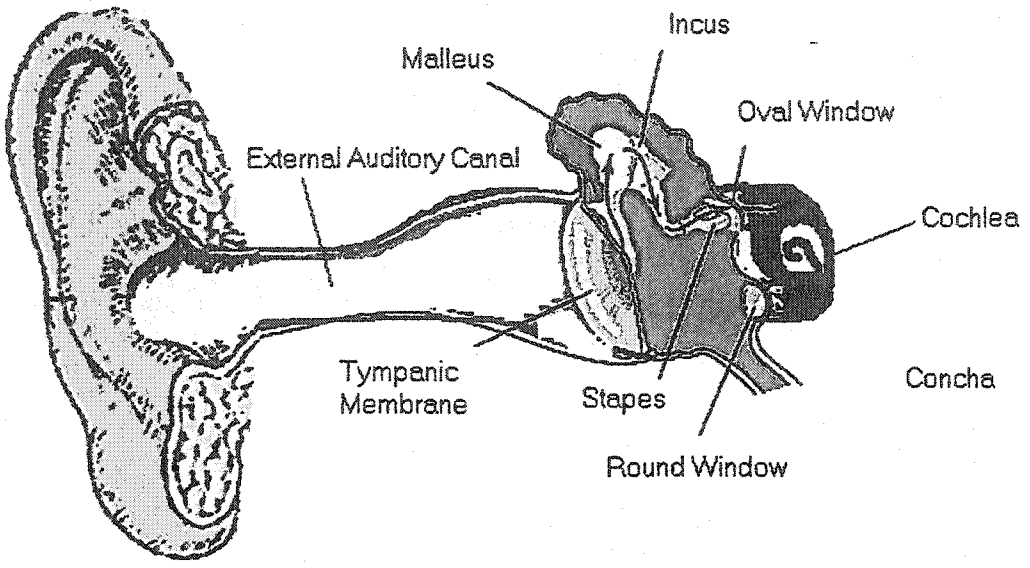

Figure 2.1 A schematic overview of the peripheral auditory system. Adapted from Encyclopaedia Britannica, 1997.

2.2 External ear

The external ear is made of the pinna and external auditory meatus. The pinna consists of a skin-covered thin plate of cartilage. It captures sound-pressure waves in open air and guides them into the external auditory canal. The latter is a narrow channel that runs forward and medial in a slightly curved course from its lateral orifice to its medial boundary. The distance from the concha of the auricle to the tympanic membrane is about 2.5 cm. The outer one third of the canal is cartilaginous, and the inner two thirds are bony. The diameter of the canal is not uniform: its vertical diameter is greatest at its lateral end, while its antero-posterior diameter is greatest at its medial end. It directs the waves towards the tympanic membrane. The epithelium of the external auditory canal is in direct continuity with the epidermal layer of the tympanic membrane.

2.3 The tympanic membrane

The membrane is connected to the bony portion of the ear canal, the tympanic ring, by means of the annular ligament. The tympanic membrane is composed of three layers: a

lateral epidermal layer, an intermediate fibrous layer, and a medial mucous layer. A cross-sectional view of the tympanic membrane is illustrated in Figure 2.2.

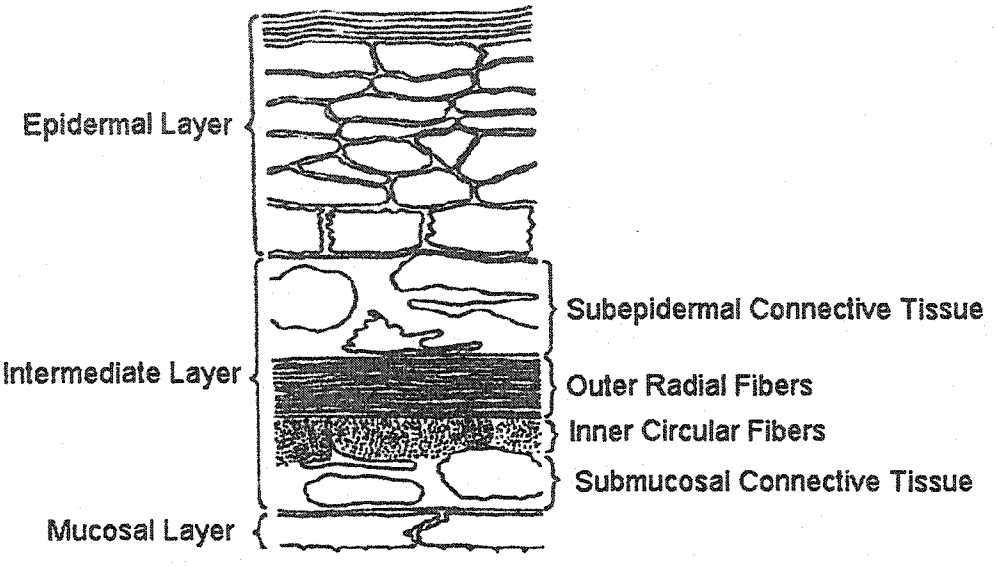

Figure 2.2 A cross sectional schematic diagram of the pars tensa of the tympanic membrane. From Funnell (1972), after Lim (1968).

The thickness of the eardrum is about 0.1 mm. Its vertical diameter along the manubrium varies from 8.5 to 10 mm and its horizontal diameter measures approximately 9 mm in diameter. The tympanic membrane is attached to the manubrium of the malleus between the lateral process and the umbo. It is divided into the pars tensa and pars flaccida or Shrapnell's membrane. The former is rich in organised radial and circumferential collagen fibers in its fibrous layer, while the latter has fewer and less organised collagen fibres. The anterior and posterior mallear folds, extending from the short process of the malleus to the annular rim, separate both areas as illustrated in Figure 2.3.

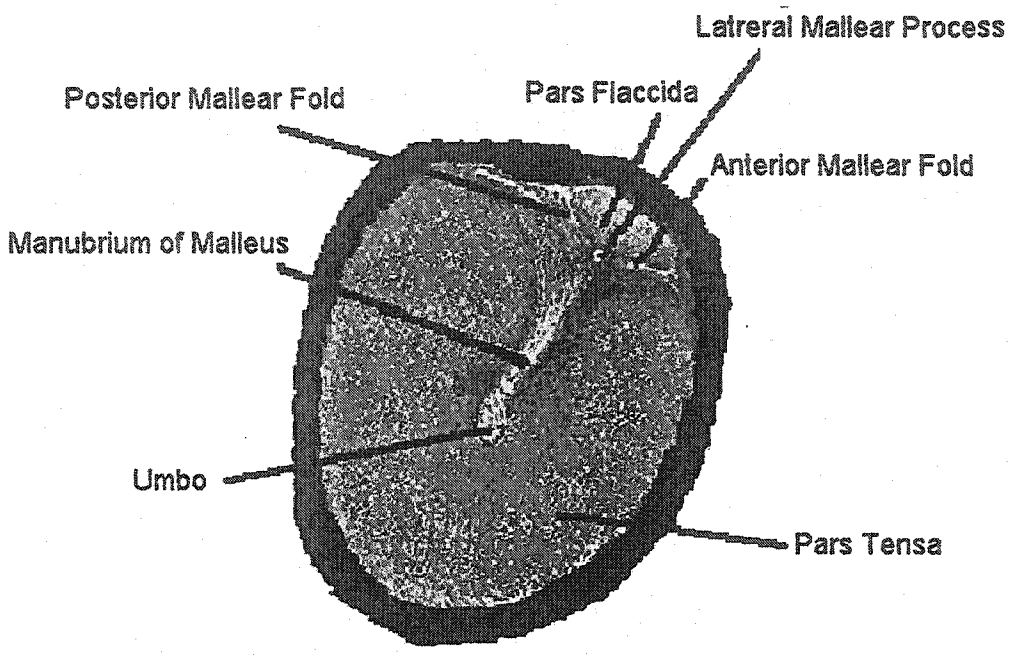

Figure 2.3 Lateral view of the tympanic membrane and the underlying ossicles. Adapted from Anson & Donaldson, 1992.

Pathological conditions of the tympanic membrane that can be studied with finite-element modelling include, amongst others, perforations and "monomeric" membrane. The latter condition occurs in situations where spontaneous healing of perforations results in a thinned transparent membrane consisting of medial and lateral layers with little intervening fibrous layer.

2.4 The middle ear

The middle-ear cleft consists of the tympanic cavity, the mastoid air-cell system, and the eustachian tube. The tympanic cavity is an air-filled space within the temporal bone that couples sound energy to the cochlea. It contains the auditory ossicles and their attached ligaments and muscles. The tympanic cavity can be schematically represented by a box, as illustrated in Figure 2.4.

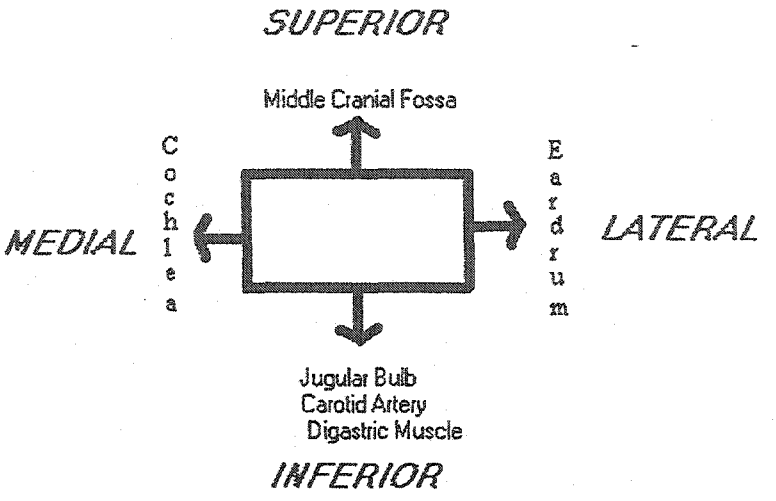

Figure 2.4 Relationship of the tympanic cavity to surrounding structures. Adapted from Wright, 1997.

The roof of the tympanic cavity is formed by the bony tegmen tympani, which separates it from the dura of the middle cranial fossa. The floor of the tympanic cavity, a thin plate of bone, separates the tympanic cavity from the dome of the jugular bulb. The middle ear is separated from the inner ear by the oval and round windows of the cochlea. The ossicular chain transfers the sound-pressure wave to the oval window and causes the liquid within the cochlea to move. Sensory cells, located in the middle chamber of the cochlea (scala media), are capable of transducing the mechanical movement of the liquid into an electrical signal, which is passed to the auditory cortex by the cochlear nerve.

2.5 The auditory ossicles and their attachments

2.5.1 Introduction

The auditory ossicles, known as the malleus, the incus and the stapes, transmit sound energy from the tympanic membrane to the inner ear. They are illustrated in Figure 2.5. In addition to delicate articular capsules that surround the joints between the auditory ossicles, there are ligaments that connect the latter to the walls of the tympanic cavity. Two muscles are also associated with the ossicles, namely the tensor tympani and the stapedius muscles. Understanding the anatomy of the ossicles and ligaments in detail is vital to thorough finite-element modelling of the middle ear, especially in clarifying the interpretation of magnetic-resonance-microscopy data sets and histological serial

sections. Each ossicle will be discussed individually along with its attached ligaments and muscles.

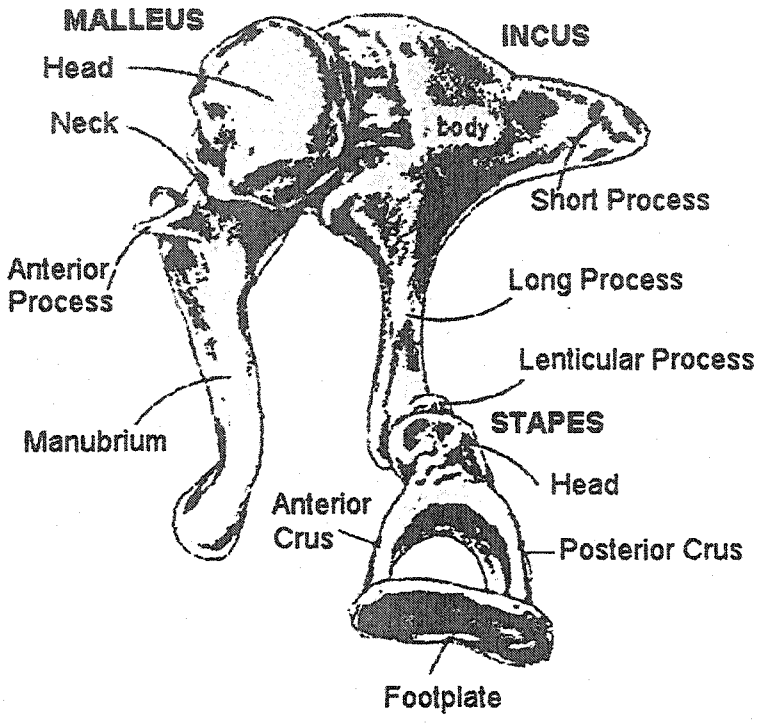

Figure 2.5 Drawing of the middle-ear ossicles. From Ladak (1993), after Anson and Donaldson (1967)

2.5.2 The malleus

The malleus is the most lateral of the three ossicles. It consists of a head, a neck, and three processes: the manubrium, an anterior process and a lateral (or short) process, as illustrated in Figure 2.5. Its overall length ranges from 7.5 to 9.0 mm (Wright, 1997). The average weight of the malleus is approximately 23 mg.

The round head lies above the level of the tympanic membrane in the epitympanic area. Its superior surface offers an attachment for the superior mallear ligament, which connects it with the roof of the tympanic cavity. The posterior surface of the head articulates with the body of the incus. The manubrium of the malleus is intimately connected with the fibrous layer of the eardrum, and is covered medially by the mucous layer. The plica mallearis is a fold of mucosa connecting the manubrium to the eardrum

along the medial curvature between the lateral process and the umbo. The lateral process protrudes laterally from the top of the manubrium, and abuts the tympanic membrane below the pars flaccida. The lateral mallear ligament connects the lateral process to the margin of the tympanic incisure. Finally, the anterior process is a projection of bone extending from the neck of the malleus forward and downward into the petrotympanic (glasserian) fissure. It connects the anterior process to the anterior wall of the tympanum, passing through the petrotympanic fissure, and can extend as far as the angular spine of the sphenoid bone. It is commonly thought that the anterior mallear ligament in concert with the posterior incudal ligament serves to establish the axis of rotation of the ossicles. It is believed that the suspensory mallear ligaments also provide stability during changes in middle ear pressure, and dampen the ossicular response during high-intensity stimuli.

One muscle attaches to the malleus, namely the tensor tympani. Its origin is the eustachian tube, the walls of the bony semicanal that encircle it, and part of the adjacent greater wing of the sphenoid. The most medial fibres of the tendon insert into the cochleariform process, while its main body turns 90 degrees laterally to insert onto the medial and anterior surfaces of the manubrium as well as part of the neck of the malleus. The tensor tympani displaces the manubrium medially, therefore decreasing the compliance of the tympanic membrane.

2.5.3 The incus

The incus is the largest of the auditory ossicles. It consists of a body, a short process, a long process and the lenticular process (often neglected in the hearing literature). The average weight of the incus is approximately 27 mg. The body lies in the epitympanum and has a cartilage-covered facet that articulates anteriorly with the posterior side of the mallear head. The saddle-shaped incudo-mallear articulation is synovial and contains a bilaminar interarticular disc. The long process descends into the mesotympanum posterior and medial to the handle of the malleus. The short process projects backwards from the body to lie in the fossa incudis, to which it is firmly anchored by the posterior incudal

ligament. The medial and lateral incudo-mallear ligaments secure the body of the incus to the head of the malleus.

The lenticular process of the incus has occasionally been described as a separate bone referred to as the "fourth ossicle"(Asherson, 1978). The lenticular plate articulating with the stapedial head is a convex surface connected to the long process of the incus by an extremely narrow pedicle. The incudo-stapedial joint is synovial in type, and has articulating surfaces lined by cartilage. The surrounding capsule provides adequate support to the joint. Recent work by Heng and Funnell (Siah, 2002; Siah & Funnell, 2001) demonstrated that most of the flexibility between the incus and the stapes might originate from the bony pedicle of the lenticular process rather than from the incudo-stapedial joint itself. A drawing illustrating the relationship of the lenticular plate to the long process of the incus is shown in Figure 2.6.

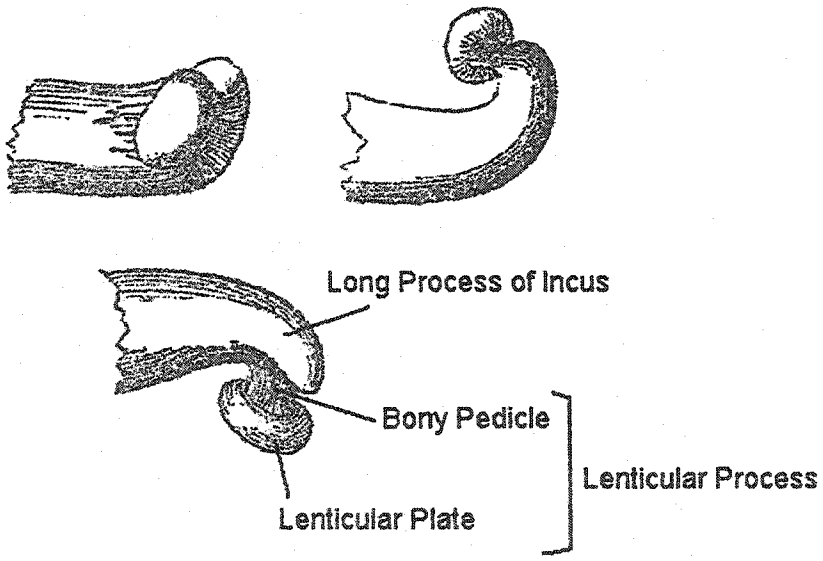

Figure 2.6 Drawing of the lenticular process of the incus. Adapted from Shrapnell, 1832.

2.5.4 The stapes

The stapes is the smallest bone in the body and weighs only 2.5 mg. It consists of a head (capitulum), a neck, two crura, and a footplate. The head points laterally and has a small

cartilage-covered depression that articulates with the convex lenticular process of the incus. Both crura are concave on their inner surfaces, but the posterior crus is thicker and more curved than the anterior one. The head, neck and two crura form the stapedial arch attaching to the footplate. The latter measures on average 3mm in length by 1.4mm in width. Its lateral surface can have a longitudinal ridge referred to as the crista stapedialis. The footplate lies within the oval window where it is attached to the bony margins of the labyrinthine capsule by the annular ligament. The stapedio-vestibular articulation is a syndesmosis that has spaces in 70% of adults (Bolz and Lim, 1972) possibly related to pressure or friction.

The stapedius muscle is contained in a bony canal in the posterior wall of the tympanic cavity. It exits at the pyramidal eminence and usually attaches at a rough area near the superior aspect of the posterior crus. Occasionally it inserts into the stapedial head. The stapedius muscle is absent in 1% of individuals. Its contraction in response to sudden loud noises drives the anterior aspect of the stapes base laterally. This is believed to protect the inner ear from acoustic trauma.

2.6 Function of the middle ear

The function of the middle ear is intrinsically complex. The classical teachings are overly simplified and misrepresent the real dynamics of the middle ear. The middle ear acts as a coupler that matches the low impedance of air to the high impedance of the liquid in the inner ear. The main transformer action results from the fact that the force produced by the acoustic pressure acting on the eardrum is applied to a much smaller surface area at the footplate. According to the classical theory, the transformer ratio has two components:

(1) One component was said to result from the ratio of the effective tympanic-membrane surface area to the surface area of the footplate. Since it was believed that 'the whole eardrum except the extreme periphery vibrates as a stiff surface along with the manubrium' the 'effective area' of the eardrum would thus simply be the area of the stiff part (Békésy, 1941).

(2) The second component was said to result from the lever ratio corresponding to the

length of the malleus (from the axis of rotation to the umbo) divided by the length of the incus (from the axis of rotation to the incudostapedial joint). Calculation of the lever ratio in this way assumes that the malleus rotates around a fixed axis, and that all the force of the tympanic membrane is applied at the umbo. This classical theory corresponded to quite a simple mechanical system, and was well represented by lumped-parameter circuit models as described below. Unfortunately, various experiments have shown that the situation is more complicated. Békésy himself observed that above 2.4 kHz 'the conical portion of the eardrum loses its stiffness, and the manubrium in its motion lags behind the motion of the adjacent portion of the membrane'. Even at low frequencies, however, the motion of the eardrum is not that of a hinged stiff plate. Khanna and Tonndorf showed this conclusively using time-averaged holography (Khanna 1970; Khanna & Tonndorf 1972; Tonndorf & Khanna, 1972). Furthermore, the ossicular rotation around a fixed axis running from the anterior process of the malleus to the posterior incudal ligament, as described by Bárány (1938) and von Békésy(1960) has been radically refuted by recent experimental measurements. Decraemer and Khanna have shown that the position of the axis of rotation changes greatly with frequency and even within each cycle of oscillation (Decraemer et al., 1991a; Decraemer & Khanna, 1992). But the reality is even more complex: by measuring mallear vibrations along the three axes x, y and z, they showed that the motion of the malleus has both rotational and translational components in each of the 3 dimensions (Decraemer & Khanna, 1995; Khanna & Decraemer, 1997).

From all these experimental measurements it becomes evident that the concept of fixed lever and area ratios is inaccurate and that middle-ear dynamics are extremely complicated. Sophisticated numerical models such as finite-element models are therefore required to quantitatively explain and accurately simulate the mechanical behaviour of the middle ear.

Chapter 3

FINITE-ELEMENT METHOD

3.1 Introduction

This section is a brief description of concepts of the finite-element method. Many textbooks have been written on the subject and provide a more exhaustive coverage of the topic (Zienkiewicz & Taylor, 2000; Carroll, 1999; Bathe, 1995).

3.2 The finite-element method

3.2.1 General principles

The finite-element method divides structures of interest into elements with a finite size, permitting the analysis of mechanical behaviour of complex structures that would not be possible otherwise. Elements can have a variety of shapes and forms such as triangles, beams, rectangles, etc. The process of dividing a region into elements is known as mesh generation. For example, a complex structure such as a stapes can be divided into a number of regular triangles, rectangles and beam elements, which together make the overall intricate shape, but are easy to analyse individually. Figure 3.1 illustrates a complex structure such as the malleus divided into a number of simple elements:

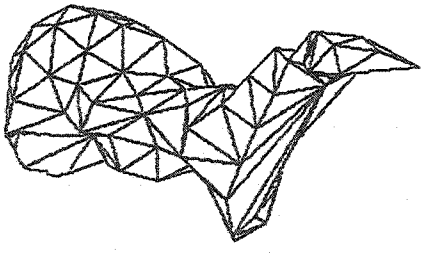

Figure 3.1 Segmentation of the malleus into simple elements.

After the structure of interest is divided into simple elements, the mechanical behaviour of each element is then analysed, and its response to specific applied loads is expressed in terms of the displacements of its edges. Elements are connected at their edges at specific

points called nodes. The mechanical response of each element is analysed based on the Ritz-Rayleigh procedure as discussed below.

3.2.2 Ritz-Rayleigh procedure

The Ritz-Rayleigh procedure is the most common tool used to formulate finite-element approximations. It was introduced by Rayleigh in 1877 and generalised by Ritz in 1908. The procedure is based on the theorem of minimum potential energy in mechanics, which states that if one obtains a functional giving the potential energy of a system, then the "admissible" function which minimises that functional is the solution of the system. An admissible function has to satisfy the boundary conditions of the boundary-value problem, as well as certain continuity conditions.

In general, a complete minimisation of the functional is difficult or impossible. Therefore, a limited set of functions will be used to minimise the functional. The Ritz-Rayleigh procedure restricts the search to a simple subset of admissible functions, that is, the space of linear combinations of n independent admissible basis functions, $W_1(x),\ldots, W_n(x)$, leading to a set of admissible functions that can be expressed as:

$$w(x) = \sum_{i=1}^{n} c_i w_i(x)$$

where the c_i are n constants defining $w(x)$.

Let $F(w)$ be the functional over this set. Minimising $F(w)$ implies that the c_i have to be chosen so that F is minimal. Taking the partial derivatives of F with respect to each c_i in turn, and setting each to zero, accomplishes this task. The result is a set of n algebraic equations in c_i: $\frac{\partial}{\partial c_i} F(\sum_{i=1}^{n} c_i w_i) = 0 \quad I=1, 2,\ldots,\ldots,\ldots,n$

Now the boundary-value problem is reduced to the solution of n linear equations in n unknowns.

The result of the element analysis is a matrix equation relating the behaviour of the element to the applied forces. Once all of the element stiffness matrices and load vectors have been obtained, they are combined into one overall structure matrix equation, which

relates nodal displacements for the entire structure to nodal loads. After applying boundary conditions, the structure matrix equation can be solved to obtain unknown nodal displacements; intra-element displacements can be interpolated from nodal values using the functions defined previously over each element.

3.2.3 Properties of the finite-element method

The finite-element method has many attractive features. It can easily handle non-linearity, irregular boundary shapes, and complex geometries. More importantly, the model can accurately represent the anatomy, physiology, and biomechanical properties of the system studied rather than rely on a circuit model with variously assigned parameters. The parameters of a finite-element model have very direct relationships to the structure and function of the system analysed, and can be estimated independently of the experimental situation being modelled.

The computational demands of a finite-element model are adjustable. Using a small number of elements permits a faster analysis but the solution obtained may not be accurate. In general, as the number of elements increases, displacements converge to true values. However, an extremely fine mesh is more computationally demanding. A good compromise is to select the coarsest mesh for which displacements are close enough to the true values. This can be found by using increasingly finer meshes while modelling the structure of interest until the results converge.

3.3 Analysis software

The finite-element analysis programme used in this thesis is SAP IV. This was first developed by Bathe et al. in 1973. SAP IV was made available as source code and has been adapted for several years for use in middle ear research (Funnell, 1978). It is written in Fortran and currently runs under Unix, Linux, and Microsoft Windows operating systems.

Chapter 4

METHODOLOGY

4.1 Introduction

This chapter outlines each of the steps of the modelling ladder. Building an accurate human middle-ear model involves obtaining accurate anatomical and geometrical data as a first step. This is achieved by utilizing information from moirė topography, magnetic resonance microscopy (MRM) and temporal-bone histology. Segmenting the data, generating a mesh, stacking the data, and devising the finite-element model follow as logical sequential steps. An algorithm illustrating the modelling process is illustrated in Figure 4.1.

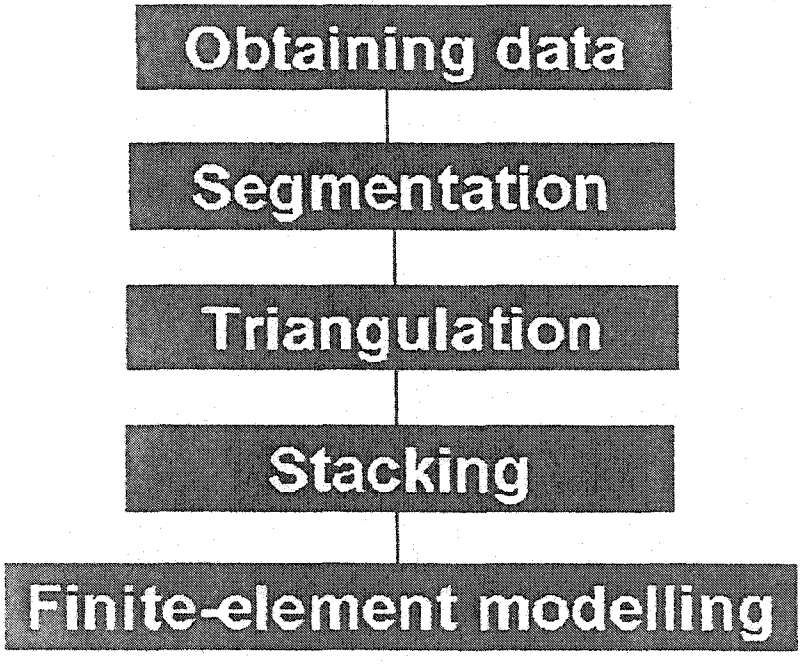

Figure 4.1 Modelling ladder with individual steps outlined.

4.2 Data Acquisition

4.2.1 Introduction

The first step in generating complex three-dimensional models is a geometrical representation of the structure of interest. The components of most relevance to the mechanics of the middle ear are the tympanic membrane, middle-ear ossicles, and ligaments. The anatomy of these structures is derived as follows.

4.2.2 Tympanic-membrane anatomy

The precise three-dimensional shape of the eardrum, with its boundary definition and displacement measurements in the presence of various static pressures applied, was obtained using phase-shift moiré topography.

4.2.2.1 Introduction

The word 'moiré' was first used by weavers and comes from the word 'mohair', a kind of fabric made from the fine hair of an Angora goat. The moiré phenomenon is seen in everyday life when two objects with periodic structures are visually superimposed. The resulting interference produces patterns of high and low light transmission referred to as moiré fringes. While initially introduced in medical research by Takasaki in 1970, to the best of my knowledge, W. Decraemer (University of Antwerp, Belgium) is the only researcher equipped with a state-of-the-art moiré interferometer that has been adapted to obtain 3-dimensional shape measurements of the tympanic membrane. The model in this thesis is the first human model to rely on such a powerful technique, as the available shape data in previous models have not been complete or precise, despite the fact that the mechanical behaviour of the eardrum is intrinsically related to its shape. While Khanna and Tonndorf were the first to use moiré topography to assess the eardrum shape using silastic castings, a quantitative analysis of their data was severely hampered by difficulties in accurately interpolating moiré fringes and by flaws in the castings near the edges (Funnell, 1979, 1981). Dirckx & Decraemer were the first to introduce measurements of the shape of the tympanic membrane without castings and without

fringes, with the use of phase-shift moiré topography (Dirckx et al, 1988; Dirckx and Decraemer, 1989). Phase-shift technique offers a non-contacting method for assessing the shape of the object of interest.

4.2.2.2 The moiré technique

Considering that the eardrum reflects poorly, application of white India ink is important to obtain a good optical contrast as the moiré technique requires a diffusely reflecting surface (Decraemer & Dirckx, 1991). The weight of the ink has proved to have negligible effect on the shape of the eardrum (Funnell & Decraemer, 1996). The first step of the moiré technique involves projecting the shadow of a grating of parallel lines onto the eardrum of a fresh temporal bone placed close behind the grating. The eardrum will cause a modification of the shadows of the grating lines, depending on its shape. When the eardrum is viewed through the line grating, the interference between the undisturbed grating and its projection generates fringes that can be interpreted as intersections of the object with a set of equidistant bright and dark planes parallel to the grating (Decraemer et al. 1991). The moiré images are recorded with a CCD camera and a frame store. Four phase-shifted images are obtained by moving the temporal bone slightly along the axis perpendicular to the grating. These images are then combined pixel by pixel to form a single image in which each pixel specifies the z coordinate of a point (Funnell & Decraemer, 1996). This highlights a basic advantage of this technique in allowing a three-dimensional representation of the external surface of interest with images produced having pixel values directly related to the z coördinates. The z values are measured with an accuracy of 0.005mm (Dirckx & Decraemer 1990). Also, since in the apparatus the image plane is parallel to the grating plane, and an orthogonal coordinate system is chosen such that the x-y plane is parallel to the grating plane, the z coordinate reflects the depth of a given point behind the grating. Another advantage to phase-shift moiré is the possibility of determining, by measurements under large static pressures, the boundaries of the pars flaccida, pars tensa, and manubrium.

Figure 4.2 shows an example of a moiré image obtained by Decraemer for one ear with no static pressure applied (p = 0). Horizontal and vertical profiles through the umbo are

shown for p=0 and for applied pressures of ±400 and ±800 Pa (±4 and ±8 cm H_2O).

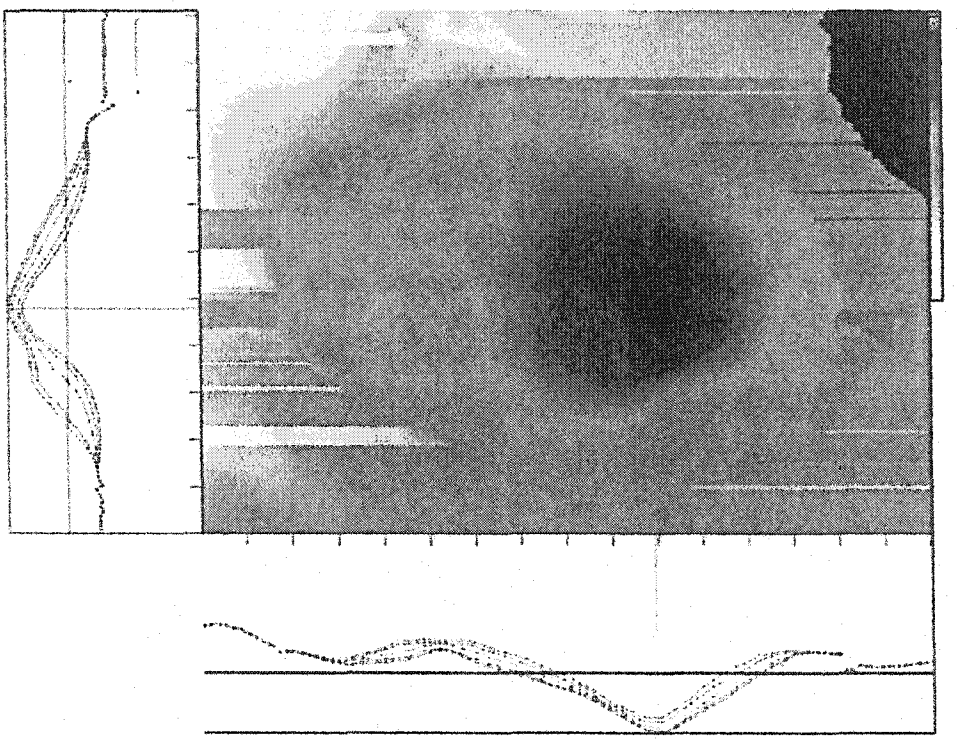

Figure 4.2. Example of a moiré image obtained by Decraemer for one ear with no static pressure applied (p = 0). Horizontal and vertical profiles through the umbo are shown on the x and y axes, respectively. These profiles are shown for p=0 (middle line) and for applied pressures of ±400 and ±800 Pa (±4 and ±8 cm H_2O). Moiré data processed by Funnell's Mum programme (Funnell & Decraemer, 1996).

The shape of the pars tensa in this model was derived from the moiré data using the same techniques previously used by Funnell for the cat and the gerbil (Funnell & Decraemer, 1996; Funnell et al., 2000). The outlines of the eardrum and manubrium are obtained from visual inspection of the shape profiles.

4.2.3 Middle-ear anatomy

4.2.3.1 Introduction

Most of the previous finite-element models of the human middle ear relied on published averages in the literature for the geometries of the various ossicles. The model presented in this thesis is unique in being the first to rely on accurate data such as those obtained with magnetic resonance microscopy and histological serial sections.

4.2.3.2 Magnetic resonance microscopy

In order to create a model with a realistic 3-dimensional geometrical shape, the anatomy of the middle-ear ossicles was reconstructed from magnetic-resonance microscopy (MRM) data sets. MRM, being developed by the Duke University Center for In Vivo Microscopy, is a powerful evolution of magnetic resonance imaging (MRI), which I was fortunate to have access to through Miriam and O.W. Henson Jr (Univ. North Carolina at Chapel Hill).

Magnetic Resonance Imaging (MRI) has become a major 3-dimensional diagnostic tool used in medicine and surgery to demonstrate anatomy and pathological changes. The main advantage of this modality over other techniques, such as x-ray CT scanning, stems from the fact that soft-tissue boundaries are clearly visualised. Another value of MRI (shared with x-ray CT) is that the true 3-D high-resolution geometry of the specimen is maintained in a non-destructive way with accurate alignment, in contrast with conventional histology where slice-to-slice alignment is a problem, and where distorted or missing sections can cause inaccuracies of the 3-D representation. Furthermore, the images are isotropic, that is, are of equal resolution in all three dimensions and can be turned on any angle, and sectioned along any plane.

Magnetic Resonance Microscopy (MRM) is based on the same physical principles as magnetic resonance imaging (MRI) and can be seen as an extension of the MRI technique carried to microscopic dimensions. It produces images with higher-than-normal spatial resolution mainly because of the use of strong magnetic field gradients (200-800 mT/m) and specialized radio-frequency (RF) coils.

Several authors have discussed the physical principles of MRM e.g., (Zhou et al., 1995; Brown et al., 1999), so only a brief synopsis will be provided here. Basically, when a collection of protons is placed in a strong magnetic field, they try to align themselves with the external field. The angular momentum causes all of the protons to precess about the magnetic field at a very explicit frequency, the Larmor frequency ω obtained by the following equation:

$$\omega = \gamma \beta_0$$

where γ is a constant. Because the collection is precessing in synchrony at ω, the vector components parallel to the magnetic field β_0 add to each other to generate a net magnetization *M*. *M* also precesses at ω and is large enough to be measured as it is made of the sum of many protons acting synchronously. If an additional magnetic field $\mathbf{B}_1$ is applied at this same frequency, *M* can be forced away from the longitudinal *(z)* axis into the transverse plane. But once in the transverse plane, *M* continues to precess, and therefore will cause a time-varying signal in any antenna through which it passes. This is the nuclear induction which forms the basis for magnetic resonance imaging. While both MRI and MRM employ powerful magnets causing hydrogen atoms in soft tissue to resonate, MRM works with a much stronger magnetic gradient and delivers images at more than 250 times greater resolution. In order to achieve the desired level of microscopic spatial resolution, intrinsic resolution limits such as linewidth broadening and diffusion have to be addressed.

The advantages of MRM over conventional light microscopy are depicted in the following table:

Magnetic Resonance Microscopy	Traditional Light Microscopy
It is non destructive	Dehydration, processing and shrinkage distort the specimen
Less time consuming	Very time consuming
Proper alignment of sections is inherent in the 3D acquisition	Problem with alignment; reference points are often required but are not very reliable
The data are digital	Data have to be digitised (potential data distortion)
Isotropic dimensions of the voxels make the data ideal for reconstruction	Less adequate data for 3-D reconstruction
Data set can be used to create sections in any desired plane	Limited by possible planes of section
The entire dataset can be viewed from any point of view in a volume-rendered image	A two-dimensional image can be obtained at best

Table 4.1 Comparison of Magnetic Resonance Microscopy data with histological serial sections.

We used for our model the MRM data of a human middle ear horizontally sectioned into 180 individual slices with a voxel sizes of about 25 μm. The ear was scanned at Duke University's Center for In Vivo Microscopy at Duke University, Raleigh, NC, USA. The MRM system was a GE Omega System with a 7.1 T, 15-cm-diameter horizontal bore superconducting magnet, with 85 gauss/cm shielded gradients. The radiofrequency coil was a Helmholtz pair 15 mm in diameter (Banson 1982). M. Henson & O.W. Henson, Jr., from the University of North Carolina at Chapel Hill, prepared this particular ear for scanning. It was chosen from among several available datasets based on its completeness. Figure 4.3 shows an example of a slice.

Figure 4.3. A representative slice from MRM data set. The malleus, incus, and stapedial crus are well visualized.

4.2.3.3 Histological serial sections

Histological examination of the temporal bone has an important role in understanding the anatomy and pathology of the middle ear. Preparation of a middle-ear histological specimen involves fixation, decalcification, embedding, sectioning, staining, and mounting. Fixation is the first step in order to prevent the disintegration of proteins. This involves immersion in fixative solution such as Formalin or Heidenhain-Susa immediately after harvesting. The latter solution provides superior cytological detail (Schuknecht, 1993). Fixation is followed by decalcification through immersion in a solution of disodium ethylenediaminetetraacetate or trichloracetic acid. This is an important step as the inorganic salts impregnated in the bony matrix render slicing of the structure difficult. Next, to allow the specimen to be sliced without distortion, the decalcifying fluid present within the tissue is replaced with paraffin or celloidin. After the specimen undergoes hardening, it is placed on a microtome and sectioned in the desired plane (vertical or horizontal). Sections are usually 20 micrometers (μm) thick. By convention, unless otherwise desired, every tenth section is stained with hematoxylin and eosin, and mounted on a glass slide.

A set of horizontal and vertical histological serial sections of the human middle ear was used to supplement the MRM data, in order to better discern the fine details of soft tissues like the ossicular ligaments and muscles. These sections were digitised and scaled. Each section is about 20 μm in thickness, and the distance between consecutive sections is approximately 200 μm. Dr Shyam Khanna from Columbia University provided the main set used. This set was digitised using a Kodak DC120 digital camera, with a resolution of 1280 x 960 pixels. Ms Clarinda Northrop of the Temporal Bone Foundation in Boston, Massachusetts kindly provided two other sets from her temporal-bone collection.

Figure 4.4 shows an example of a histological section of the human middle ear. These histological serial sections were very useful in complementing the MRM data. Specifically, histology was important in defining the exact origins, insertions and dimensions of the ligaments, as well as viewing the details of the incudostapedial joint. However, in this model, histology was not used for the actual 3-D reconstruction of the model, mainly because of the alignment problem, which is not an issue with the MRM data.

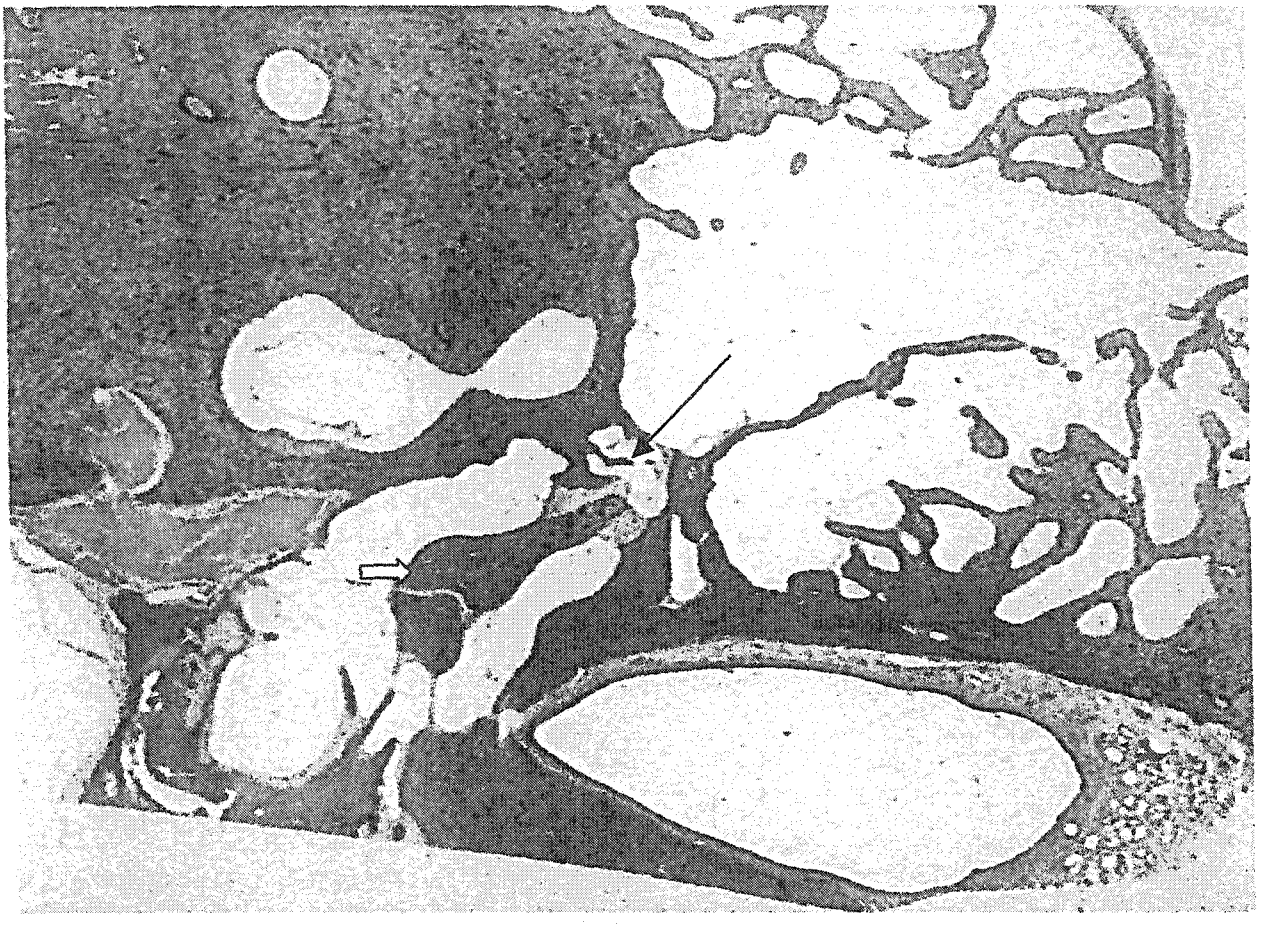

Figure 4.4 An example of a histological section of the human middle ear. The black arrow points to posterior incudal ligament, the white arrow points to the head of the malleus.

4.3 Segmentation

Segmentation of an image refers to the process of marking regions of interest in that image.

While there are numerous commercially available programs that rely on thresholding techniques to segment regions of interest, the model in this thesis is based on a tedious manual segmentation process. Manual segmentation was selected because the structures of interest are very fine, and the boundaries between different structures can be difficult to distinguish at times. Segmentation algorithms are often based on two properties of grey-level values: discontinuity and similarity (Gonzalez & Woods, 1993). Using these properties alone based on the current MRM data sets leads to errors resulting from poor

threshold separation at tissue interfaces. This is also where histology becomes useful in providing anatomical details and dimensions.

Each digitised slice was imported into a locally developed computer programme, Fie (i.e. Fabrication d'Imagerie Extraordinaire), and manually processed. Anatomical structures of interest were individually delineated and their contours were colour-coded consistently from slide to slide. For the finite-element model, the eardrum, ossicles, muscles and ligaments were included. Fie is a powerful tool that can perform image-editing and related tasks (Herrera et al., 1997). It runs readily under Unix, Linux, and Microsoft Windows operating systems and is freely available for download from the following site: *http://funsan.biomed.mcgill.ca/~funnell/AudiLab/sw/fie.html*. One drawback is the labour load related to manual tracing of boundary edges of interest. Images have to be in TIFF or raw format, and the output is a text file (.TR3) containing information on the various segmented structures in the form of nodal points of contours. Fie is able to handle both open and closed contours. A closed contour completely surrounds the structure of interest, while an open contour, as its name implies, is open and therefore is useful at the intersection of different structures and in thin structures such as the tympanic membrane, which is represented as a single layer. An example of segmentation with Fie is shown in Figure 4.5 below.

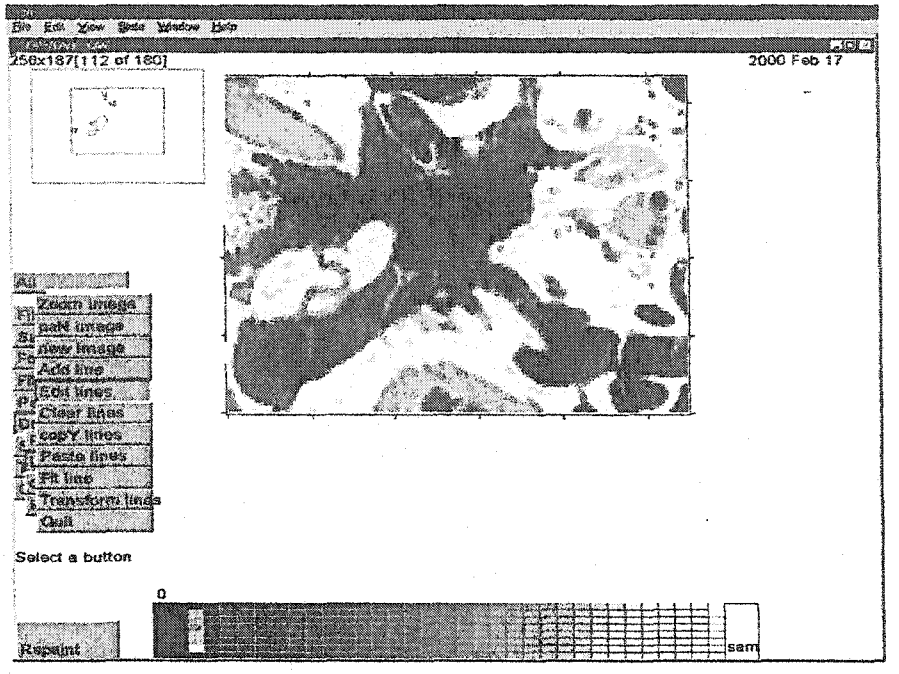

Figure 4.5 A screen shot from the Fie program illustrating the segmentation of the malleus, incus and stapedial footplate.

4.4 Triangulation

The segmented contours are then imported into a locally designed three-dimensional triangulation programme (Tr3). This software generates a mesh over each segmented structure; the mesh can be used for either visualization or finite-element analysis. The programme, under development since 1982, is capable of triangulating 3-D surfaces between serial-section contours (Funnell, 1984a,b). It utilizes the .tr3 plain-text model-definition files generated by Fie and produces, among other output files, a finite-element model file (.sap). The Tr3 programme, which runs under Unix, Linux, and Microsoft Windows operating systems, is available for free download at:

http://funsan.biomed.mcgill.ca/~funnell/AudiLab/tr3.html

The mesh is created by optimally connecting contours in neighbouring slices with triangles. The generated finite-element mesh consists of triangular thin-shell *elements*. This is justified for thick structures such as the ossicles by the assumption that as long as the structure undergoes rigid-body motion only, no stresses or strains are induced within the structure.

Each *element* is a triangle of arbitrary geometry and each of its vertices has six degrees of freedom, namely three rotational and three translational. Each small triangle is assigned mechanical properties such as material stiffness (Young's modulus) and boundary conditions (free or clamped), as well as other parameter properties as illustrated in Table 4.2. A decision is made as to how many elements should represent the structure, for example, into how many small triangles the stapes footplate should be divided. The finer the mesh, the more accurate is the representation of the structure. Unfortunately, the greater the number of elements in the structure, the greater the amount of time needed to solve all the equations in the system. Thus, a very fine mesh is computationally very demanding. A very coarse mesh would consume much less time, but the displacements of the model would not be as accurate. Therefore, it is important to find an appropriate mesh resolution for the model. One way to decrease the computational time is to minimize the size of the bandwidth of the stiffness matrix, i.e. the width of the band of non-zero numbers that lie about the diagonal of the stiffness matrix. A local programme (Funnell, 1983) has been used to that effect. It renumbers the nodes using the algorithm of Crane et al. (1976) and determines a rearrangement of rows and columns that will lead to a rearranged matrix with a smaller bandwidth and profile. Figure 4.6 below illustrates triangulation of the malleus as generated by Tr3.

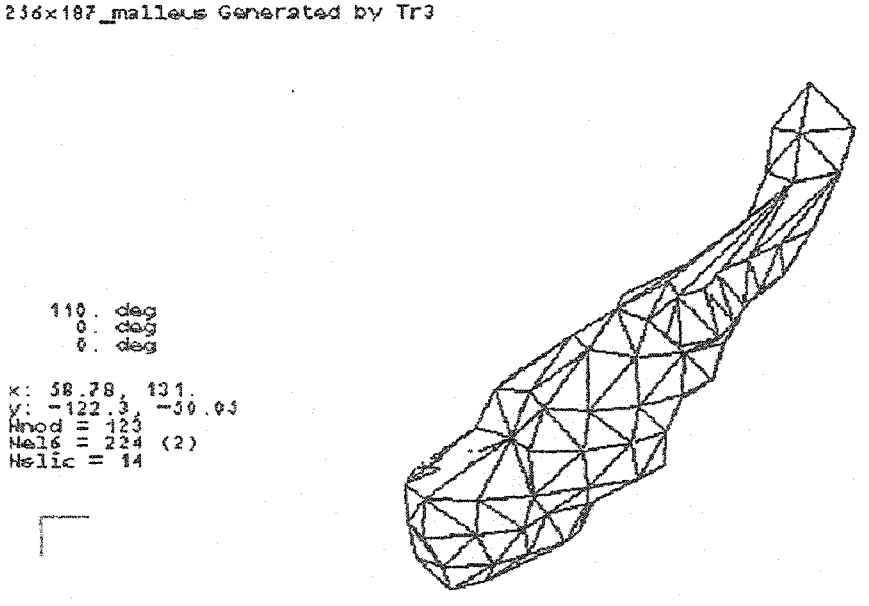

Figure 4.6 Triangulated surface of the malleus as generated by Tr3 programme.

Table 4.2 illustrates the various parameters that can be set within the Tr3 file.

Parameters	
-op [*type*]	Specifies an open contour [OP], as opposed to a closed contour [CL]
-c [*colour*]	Various structures are assigned different colours: 1 white, 2 red, 3 green, 4 blue, 5 cyan, 6 magenta, 7 yellow, 0 black.
-r [*el/d*][*spacing*]	Sets the parameters for the triangulation. [*el/d*] is the nominal number of elements per diameter and [*spacing*] is the parameter which sets the spacing between the slices which are analysed in the triangulation.
-t [*transparency*]	Sets the transparency for the VRML output of the Tr3 programme. [*transparency*] 1 is defined as transparent and 0 as opaque.
-b [*boundary*]	Sets the boundary condition. [*boundary*] may be assigned a C for clamped or F for free.
-m [*material*] [thick]	Sets the material type and thickness.
-p [*pressure*]	This is a multiplier that sets the pressure on a structure by multiplying by a model-wide pressure value.
-s [*slocation*]	Establishes a connection between contours. -s is used to link the starting node of the contour to a node of another contour. This can be the nearest, last or first node of the other contour using n, s or f, respectively.
-f [*flocation*]	Establishes a connection between contours. -f is used to link the finishing node of the contour to a node of another contour.

Table 4.2 Definition of parameters within the Tr3 Header.

4.5 The finite-element model

The triangulated surface produced by Tr3, excluding the eardrum, is combined with the triangulated surface for the eardrum derived from the moiré data to produce a combined finite-element model of the human middle ear.

The pars tensa is modelled as a uniform, homogeneous curved shell with a Young's modulus (material stiffness) of 20 MPa and a density of 10^3 kg m^{-3}. The thicknesses of the pars tensa and of the pars flaccida were determined from our histological sections to be 100 μm and 200 μm, respectively. The Young's modulus of the pars flaccida has been taken as one tenth that of the pars tensa. The acoustical input is a uniform sound pressure of 1 Pa. A finite-element programme, SAP IV, then computes all of the element stiffness matrices and load vectors and combines them into an overall system matrix equation. This

overall equation can then be solved to give the middle-ear displacements resulting from the applied sound pressure.

Chapter 5

RESULTS

5.1 Introduction

The following section presents the results of simulations carried out with the model using the methodology described above. The model consists of the tympanic membrane, malleus, incus, stapes, tensor tympani, stapedius, anterior mallear ligament and posterior incudal ligament.

5.2 Normal middle-ear simulation

Once the normal human middle-ear model was compiled as described in the methodology section, various simulations were conducted. For example, Figure 5.1 below illustrates a medial and a lateral view of a simulation with the model. The simulation in this case was conducted at low frequencies (i.e., frequencies low enough that inertial and damping effects are negligible). Displacements in this figure are qualitatively illustrated on the coloured side scale with smaller displacements coded in darker colours (black < blue) and larger displacements in lighter colours (green < yellow).

Figure 5.1 Lateral (top figure), and medial (bottom) views of the combined finite-element model derived from both moiré data (eardrum) and MRM data (ossicles & ligaments). Colour coded to represent calculated displacement amplitudes.

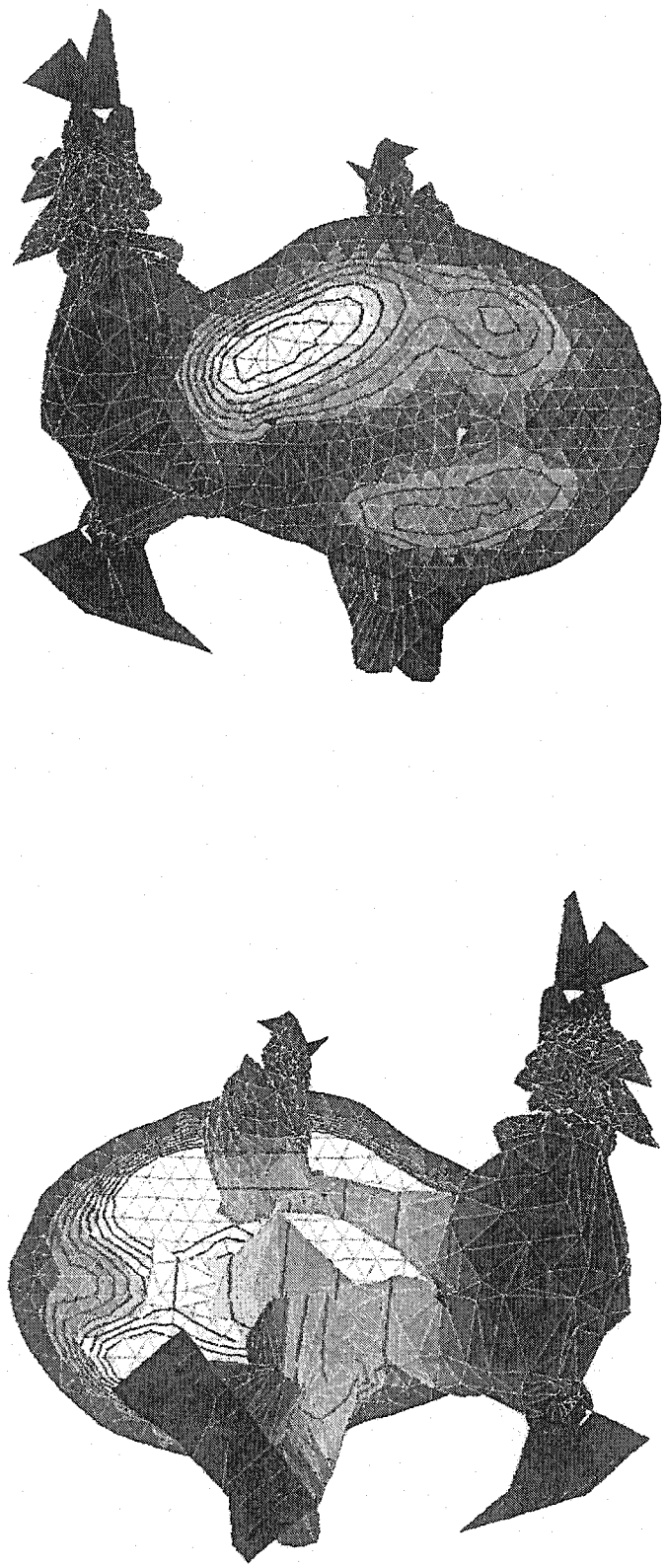

The model demonstrates the following points, which have been validated experimentally by various studies.

With regard to the eardrum, while it was believed that 'the whole eardrum except the extreme periphery vibrates as a stiff surface along with the manubrium', it is clearly shown by the model that, even at low frequency, the tympanic membrane does not move as a stiff plate; rather more displacement occurs postero-superiorly and antero-inferiorly. This is in accordance with experimental studies such as those of Khanna and Tonndorf demonstrating asymmetrical movement of the eardrum using time-averaged holography (khanna & Tonndorf, 1972).

The model also demonstrates details of displacements of the ossicles. For example, the motion of the stapedial footplate, while generally thought to have a piston-like movement, clearly has a rocking nature in this model as illustrated in Figure 5.1 by the spectrum of colours illustrating variable displacement at the footplate.

From the above findings it is apparent that a finite-element model is able to qualitatively and quantitatively address the complex mechanical behaviour of the middle ear. A "lumped-circuit" model would not have been able to address such aspects of the behaviour of the middle ear.

5.3 Simulation of incus erosion

The versatility of the model allows simulation of such conditions as incudal erosion. This condition can occur clinically in the setting of necrosis secondary to trauma or destruction by tumour or cholesteatoma. Depending on the specific pathology and ossicular discontinuity, the latter can have various effects on stapedial footplate motion. A simulation of incudal erosion at the level of the short process was carried out by removing the posterior incudal ligament from the model. The effect of such a simulation on the body of the incus is illustrated qualitatively in Figure 5.2. This was the first simulation of incudal erosion conducted with the finite-element method. I presented the results at the 23rd Association for Research in Otolaryngology meeting in Florida (Abou-Khalil et al., 2000).

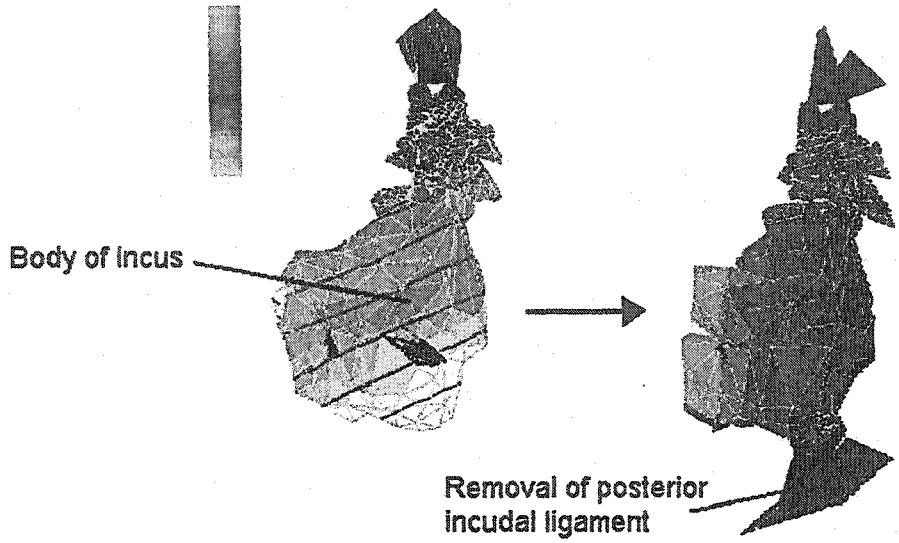

Figure 5.2 Medial view of a finite-element simulation of incudal body motion prior (left figure) and following (right figure) a simulation of short-process erosion. A decrease in the motion of the incus body can be appreciated as evidenced by the colour change. Lighter colours illustrate larger displacement.

As can be seen in Figure 5.2, a decrease in body of incus displacement occurs following removal of the posterior incudal ligament. This in effect is similar to a short process erosion disconnecting the ligament attachment.

The versatility of the finite-element model is such that a myriad of other pathological conditions affecting the ossicles can be very simply modelled and their effect on ossicular (including stapedial footplate) motion calculated, as illustrated in the following simulation.

5.4 Simulation of anterior mallear ligament fixation

5.4.1 Background

It is well known that many patients do not close their air-bone gap to within 10 dB after stapedectomy. The exact percentage varies depending on individual series. Findings at

exploration include acentric prosthesis, adhesions, and necrosis of the long process of the incus (Pederson, 1994). In Langman's series 41% of failures were attributed to erosion of the incus, while displacement of the prosthesis from the incus and migration of the prosthesis from the center of the oval window accounted for the rest (Langman, 1993).

While some authors attribute some of the failures to certain surgical techniques, we have all encountered cases where the surgical technique was outstanding and the anatomy of the patient ideal, yet we remain puzzled with a greater than 10 dB post-operative air-bone gap. One potential explanation in these cases could be a missed malleus fixation interfering with adequate ossicular sound conduction. Guilford and Anson in 1967 were pioneers in emphasizing the importance of checking for a fixed malleus in stapedectomy patients to avoid the disappointment of persistent conductive hearing loss. Ayache reported on a retrospective review of about 300 stapedectomies outlining concurrent pathological conditions encountered during stapedectomies for otosclerosis. In his series 1% of patients had a fixed malleus (Ayache, 1999). Lippy has found, in patients with malleus fixation in addition to stapes fixation, that if only stapedectomy is addressed then 30% of the patients do not close within 10 dB of their pre-operative bone conduction hearing level (Lippy, 1978).

Malleus fixation can occur at various locations, the most common being in the epitympanum. In over 1100 temporal bones studied by Subotic et al. only 14 cases of bony fixation of the malleus were found. The most common site of fixation was the lateral epitympanic wall, followed by fixation at the epitympanic roof. Fixation varied from a thin bony lamella to a thick bony bridge. Other forms of fixation include ossification of the anterior or superior mallear ligaments (Moon & Hahn, 1981). Fixation of the malleus can also occur with incomplete differentiation of the sphenomandibular ligament, resulting in a bony spicule from the anterior mallear head to the anterior tympanic fissure.

When I started working on the model in 1999, a controversy constantly brought up at Otolaryngology meetings caught my attention. It centred around the effect of anterior

mallear ligament fixation on conductive hearing loss, particularly in stapedectomy patients. Professor Ugo Fisch was proposing at the time that "hyalinisation of the anterior mallear ligament" was responsible for as many as 38% of functional failures in revision stapedectomy cases and therefore was advocating an aggressive approach towards the anterior mallear ligament (Fisch 1999). On the other hand, The Massachussetts Eye and Ear Institute group questioned the importance of the anterior mallear ligament fixation compared with another potential cause of failures in Fisch`s series, that is, the use of a 0.4mm diameter piston rather than 0.6mm (discussion period at the 2nd international symposium on middle-ear research and otosurgery, and personal communication at ARO with S. Merchant). At the time, no study in the literature had determined the effects of anterior mallear ligament (AML) fixation on middle-ear mechanics. Since the finite-element model of the human middle ear detailed in this thesis is ideal to test such an effect, I decided to use this model in order to assess the effect of AML fixation on the mechanics of the middle ear.

5.4.2 Simulation results

The finite-element model simulation of anterior mallear ligament fixation (AML) is illustrated in Figure 5.3 below. Displacements are depicted qualitatively with smaller displacements coded in darker colours and larger displacements in lighter colours.

The effect of AML fixation, with an otherwise normal middle ear and tympanic membrane, is clearly seen in the figure below. AML fixation translates into a stiffening of the entire ossicular system. Calculation of the effect on the stapes footplate, after fixating the anterior mallear ligament with all other parameters remaining intact, demonstrates a decrease in the stapedial footplate motion by a factor of 3. This corresponds to about 10 dB of hearing loss. The effect is large enough to explain some residual loss after stapedectomy.

Figure 5.3 Medial views of the combined finite-element model derived from both moiré and MRM data of a normal human ear (top figure) and one with anterior mallear ligament fixation as sole abnormality (bottom figure).

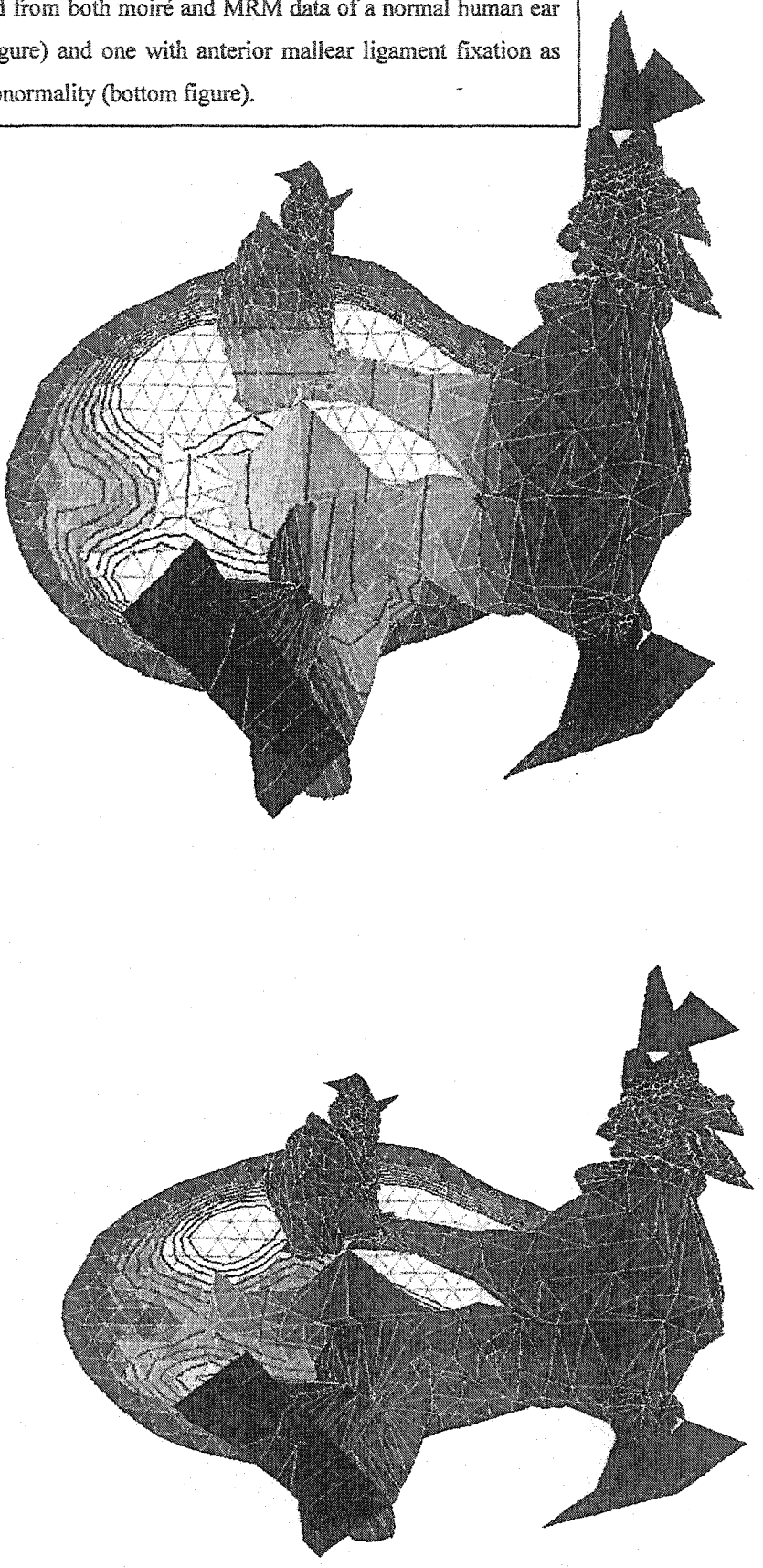

The effect of anterior mallear ligament fixation on auditory mechanics was assessed for the first time with this model. I presented preliminary results at the Association for Research in Otolaryngology meeting in 2000, and a more detailed model at the Eastern Section Meeting of the Triological Society in 2001 (Abou-Khalil *et al.*, 2000 a, 2001). Interestingly, Huber has more recently addressed the issue with experimental measurements and found an attenuation of the stapes displacement due to an isolated fixation of the AML to be in the range of -15dB (Huber *et al.*, 2001). This is certainly very consistent with our simulation of anterior mallear fixation predicting a 10-dB hearing loss at low frequencies.

Chapter 6

CONCLUSION AND FUTURE WORK

6.1 Summary

A unique finite-element model of the human eardrum and middle ear was developed. It uses exact anatomical data derived from moiré shape measurements of the tympanic membrane, histological serial sections, and high-resolution magnetic-resonance images. Moiré data provide exact shape measurements for the tympanic membrane, while the histological serial sections and the magnetic-resonance microscopy provide detailed data for ossicular, ligamentous and muscular anatomy.

Various pathological simulations were carried out in order to investigate, amongst others, the effect of anterior mallear ligament fixation on middle ear mechanics. AML fixation was found to stiffen the ossicular system, and decrease stapedial footplate displacement by a factor of three. The corresponding 10 dB of hearing loss could explain some residual loss after stapedectomy.

6.2 Limitations of the model

The main drawback of many previous ear models stems from the fact that the modelled normal ears do not behave the same way as pathological ears. This does not apply to our model. In fact the strength of our model stems from the ability to modify the variables in the system in order to precisely mimick any pathological condition desired, and therefore predict its behaviour.

Areas for improvement include automating the segmentation process as the latter is labour intensive, and different parts of the current system could be made more user-friendly. Furthermore, the current model neglects inertial and damping effects and assumes a low-frequency input. Running simulations for higher frequencies would require more information about the structure and would swell the complexity of the model because the damping and inertia of the system would have to be taken into account. However, this is an active area of research and more data should be available in

the near future.

Finally, in the current model, solid structures are modelled using shell-elements generated by the surface triangulation programme Tr3. As stated by van Wijhe, "this representation does not effectively characterize solid structures" (van Wijhe, 2000). A more realistic modelling of solid structures' behaviour necessitates the creation of volume meshes. The latter are obviously more computationally demanding and more complex to generate.

6.3 Future applications

This finite-element model can have numerous future applications. Some of the topics are briefly discussed below.

6.3.1 The design of ossicular prostheses

Reconstruction of the ossicular chain has always been a challenge to the otologist. An ideal prosthesis should be stable, easy to insert, and most importantly yield optimal sound transmission. The plethora of prostheses available bears witness to our ongoing search for the perfect solution. Numerous devices have been shown to be successful in individual series but no single technique has gained universal acceptance. This is due to the lack of uniform criteria for measuring success, the paucity of direct comparisons between various techniques, and the limited number of long-term prognostic analyses (Chole, Skarada, 1999). Furthermore, there has been little or no theoretical analysis of the mechanical performance of any of the prostheses currently available on the market. Recently, human middle-ear modelling has increasingly become a focus of attention, particularly amongst groups interested in prosthesis design and new surgical reconstructive techniques. However, the attempts at analysis that are being made are severely limited by the crudeness both of the theoretical models and of the measurements (typically impedance or single-point displacements) on the experimental models.

Finite-element models provide the only way of analysing ossicular prosthesis issues, which depend upon realistic representations of anatomy and material properties. The main

advantage of such models is the ease of manipulation of parameters, and the exact representation of the eardrum and middle-ear anatomy, allowing individualization of the treatment. Furthermore, the model allows us to import currently available prostheses and to couple their behaviour to the mechanics of the middle ear. This permits evaluation as well as direct comparisons between the various currently available prostheses in order to determine which one would be the best fit for a particular setting.

Some examples of design issues that will be addressed in the future using this model include assessing the characteristics that affect the performance of prostheses, such as shape, mass and material properties; the importance of reproducing the normal eardrum-ossicular coupling or ossicular suspension; the nature of the point of contact between the head of the prosthesis and either the manubrium or the tympanic membrane itself; and whether flexibility could be used to improve their effectiveness.

While experimental work could answer parts of these questions, this would be very expensive, as each change in a given parameter would necessitate an extra costly experiment. Furthermore, the conditions from one experiment to the next can never be exact, due to the inherent variations in middle-ear anatomy among and within different species. Nonetheless, it is evident that experiments play a major role in validating the results of a particular model.

6.3.2 Improving our screening armamentarium

The importance of hearing screening in newborns is being increasingly recognized (Mehl, Thompson 1998). While otoacoustic emissions (OAE) detection has become a popular tool for this purpose, it cannot by itself make the important distinction between conductive and sensorineural hearing loss. Tympanometry is a possible tool for the differential diagnosis but it is neither sensitive nor specific for newborns (Black et al., 1990). There is some evidence that high-frequency and/or wideband measurements may provide an effective test for newborns but considerable research is still required

(Margolis, 1997, 1998). Finite-element modelling of the acoustics and mechanics of the newborn middle ear will make it possible to extract more diagnostic information from impedance and reflectance measurements and can also contribute towards developing improved diagnostic tools. This stems from the fact that an accurate model will predict what happens to the pliable external auditory canal and tympanic membrane of the newborn from a dynamic and biomechanical perspective making it easier to understand the output of the system.

6.3.3 Assessing the influence of diseases on hearing

Three-dimensional finite-element models can simulate various clinical conditions by modifying parameters in the model. This includes, amongst others, ossicular erosion or fixation, sclerosis of the ossicular ligaments, and study of the acoustical effects of perforations in different locations of the tympanic membrane. An example is fixation of the anterior mallear ligament affecting the magnitude of ossicular displacement.

6.3.4 Pre-operative planning & post-operative assessment

Currently the ossicular replacement prosthesis is often chosen in the operating room depending on what the exploratory tympanotomy reveals and on the available prosthetic models. Our long-term aim is to be able to obtain a high-resolution CT scan of the affected individual's ear, import the images into our finite-element model and generate an individualized model. The model will then help to determine the most suitable prosthesis in terms of material properties and geometrical shape, and predict the sound transmission capacity that can be obtained. A complete model may also help to understand the surprisingly good performance of some ears after surgery and the surprisingly poor performance of others.

6.4 Conclusion

The currently designed model is unique in that it is the first human middle-ear model that uses very precise anatomical data obtained from a combination of phase-shift moiré shape measurements, histological serial sections and magnetic-resonance-microscopy data. The

model allows us not only to visualize the mechanics of the middle ear but also to change variables in the system (eroding ossicles, adding prostheses, etc.) to see how this will affect the dynamics of the system. We can therefore appreciate the importance of this model not only in terms of understanding the mechanics of the human middle ear, but also for its clinical applications.

I can foresee that this model will have major impact in hearing research in the long term as it allows us to better understand the mechanics and acoustics of the middle ear, and thus to devise better ossicular prostheses based on bio-mechanical properties of the middle ear and to individualize the treatment and screening of patients according to their anatomy.

References

Abou-Khalil S*, Funnell WRJ, van Wijhe RG, et al.(2000a): Finite-element modelling of the human eardrum and middle-ear, The Association for Research in Otolaryngology 23rd Annual Mid-Winter Meeting, St. Petersburg Beach, Florida. (*S.J. Daniel)

Abou-Khalil S*, Funnell WRJ, Zeitouni AG, Schloss MD & Rappaport J (2000b): Clinical applications of a finite-element model of the human middle ear. 54th Ann Mtg Can Soc Otolaryngol Head & Neck Surgery. (*S.J. Daniel)

Abou-Khalil S*, Funnell WRJ, Zeitouni AG, Schloss MD & Rappaport J (2001): Finite-element modeling of anterior mallear ligament fixation. Eastern Section Meeting, Triological Society, Toronto. (*S.J. Daniel)

Anson BJ, Donaldson JA (1967): The Surgical Anatomy of the Temporal Bone and Ear. Philadelphia, WB Saunders. Page 62.

Anson BJ, Donaldson JA (1992): Surgical Anatomy of the Temporal Bone. Philadelphia, WB Saunders. Page 60.

Asherson N (1978): The fourth auditory ossicle: fact or fantasy? J Laryngol Otol. 92(6):453-65.

Ayache D, Sleiman J, TchuenteAN, Elbaz P (1999): Variations and incidents encountered during stapes surgery for otosclerosis. Annales d'oto-laryngologie et de chirurgie Cervico-Faciale. 116(1):8-14.

Ball GR, Huber A, Goode RL (1997): Scanning laser doppler vibrometry of the middle ear ossicles. ENT- Ear, Nose & throat Journal. 76(4): 213-222.

Banson ML, Cofer GP, Black R and Johnson GA (1992): A probe for specimen magnetic resonance microscopy. Invest. Radiol. 27, pp. 157–164.

Bárány E (1938): A contribution to the physiology of bone conduction. Acta Oto-Laryngol. Suppl 26.

Bathe KJ, Wilson EL, Peterson FE (1973): SAP IV. A structural analysis program for static and dynamic response of linear systems. Report No. EERC 73-11, University of California, Berkeley

Bathe KJ (1995): Finite Element Procedures, Prentice-Hall, Englewood Cliffs, 1037 pp.

Beer HJ, Bornitz M, Drescher J, et al. (1997): Finite element modelling of the human eardrum and applications. Middle ear mechanics in research and Otosurgery. Proceedings of the International Workshop on Middle Ear Mechanics in Research and Otosurgery. Dresden, Germany: Karl-Berndt Huttenbrink, 40-47.

Békésy Gv (1941): On the measurement of the amplitude of vibration of the ossicles with a capacitative probe. Akust. Zeitschr ; 6: 1-16.

Békésy Gv (1960): Experiments in hearing. McGraw-Hill, New York.

Black N, Sanderson CFB, Freeland AP, et al.(1990): A randomised controlled trial of surgery for glue ear. Brit Med J; 300: 1551-1556.

Blaney AW, Williams KR, Rice HJ (1997): A dynamic and harmonic damped finite element analysis model of stapedotomy. Acta Oto-Laryngologica; 117(2):269-73.

Bolz EA, Lim DJ (1972): Morphology of the stapediovestibular joint. Acta Otolaryngol. 73(1): 10-7.

Brown BH, Smallwood RH, Barber DC, Lawford PV, Hose DR (1999): Medical physics and biomedical engineering. Institute of Physics publishing, Bristol and Philadelphia.

Carroll W F (1999): A Primer for Finite Elements in Elastic Structures, J. Wiley & Sons, New York, 512 pp.

Chole RA, Skarada DJ (1999): Middle ear reconstructive techniques. Otolaryngology Clinics of North America; 32(3):489-502.

Crane Jr. HL, Gibbs NE, Poole Jr. WG, Stockmeyer PK (1976): Algorithm 508. Matrix bandwidth and profile reduction. ACM Trans. Math. Software 2, 375-377, Complete source in "Collected Algorithms" from ACM.

Decraemer WF, Khanna SM, Funnell WRJ (1991a): Malleus vibrations mode changes with frequency. Hear. Res.; 54: 305-318.

Decraemer WF, Dirckx JJ, Funnell WRJ (19991 b): Shape and derived geometrical parameters of the adult, human tympanic membrane measured with a phase-shift moire interferometer. Hear. Res.; 51(1):107-21.

Decraemer WF, Khanna SM(1992): Modelling the malleus vibration as a rigid body motion with one rotational and one translational degree of freedom. Hear. Res.; 72: 1-18.

Decraemer WF, Khanna SM (1995): Malleus vibration modelled as a rigid body motion. Acta Oto-Rhino-Laryngologica Belgica; 49: 139-145.

Dirckx JJJ, Decraemer WF (1990): Automatic calibration method for phase shift shadow moiré interferometry. Appl. Opt. 29, 1474-1476.

Fay JP, Puria S, Steele CR (1999): Cat tympanic membrane: Annular plate and cone of strings model results in standing and travelling waves. 23rd Midwinter Res. Mtg., Assoc. Res. Otolaryngol., St. Petersburg Beach

Fisch U, Melik MD, Linder T (1999): Results of stapedectomy: are they as good as we think? The second international symposium on middle-ear mechanics in research and otosurgery, Massachusetts Eye and Ear Infirmary, Boston.

Frankenthaler R, Moharir V, Kikinis R, et al. (1998): "Virtual otoscopy" Otolaryngology Clinics of North America, 31 (2):383-392.

Funnell WRJ (1972): The acoustical impedence of the guinea-pig middle ear and the effects of the middle-ear muscles. M. Eng. Thesis, McGill University, Montreal.

Funnell WRJ (1975): A theoretical study of eardrum vibrations using the finite element method. Ph.D. Thesis, McGill University, Montreal.

Funnell WRJ, Laszlo CA(1978): Modeling of the cat eardrum as a thin shell using the finite-element method. J Acoust Soc Am; 63: 1461-1467.

Funnell WRJ, Laszlo CA (1982): A critical review of experimental observations on ear-drum structure and function. ORL; 44: 181-205.

Funnell WRJ (1983): On the undamped natural frequencies and mode shapes of a finite-element model of the cat eardrum. J.Acoust.Soc.Am.; 73, 1657-1661.

Funnell WRJ (1984a): On the choice of a cost function for the reconstruction of surfaces by triangulation between contours. Comp. & Struct., 18, 23-26.

Funnell WRJ (1984b): On the calculation of surface areas of objects reconstructed from serial sections. J. Neurosci. Meth., 11, 205-210.

FunnellWRJ, Decraemer WF, Khanna SM (1987): on the damped frequency response of a finite-element model of the cat eardrum. J.Acoust.Soc.Am.; 81, 1851-1859.

Funnell WRJ, Khanna SM, Decraemer WF (1992): On the degree of rigidity of the manubrium in a finite-element model of the cat eardrum. J. Acoust. Soc. Am.; 91, 2082-2090.

Funnell WRJ, Decraemer WF (1996): On the incorporation of moiré shape measurements in finite-element models of the cat eardrum. J. Acoust. Soc. Am.;100: 925-932.

Funnell WRJ, Decraemer WF, von Unge M, et al. (2000): Finite-element modelling of the gerbil eardrum and middle-ear, The Association for Research in Otolaryngology Annual Mid-Winter Meeting, St. Petersburg Beach, Florida.

Gonzalez RC, Woods RE (1993): Digital Image Processing. Addison Wesley, 413-478

Guilford FR, Anson BJ (1967): Osseous fixation of the malleus. Trans Am Acad Ophthalmol Otolaryngol.;71(3):398-407.

Henson MM, Henson OW Jr, Gewalt SL, et al. (1994): Imaging the cochlea by magnetic resonance microscopy. Hearing Res.;75: 75-80.

Henson OW Jr, Hazel TA, Henson MM (1999): Comparative analysis of the vertebrate ear using magnetic resonance microscopy. The Association for Research in Otolaryngology Annual Mid-Winter Meeting, St. Petersburg Beach, Florida.

Herrera DG, Maysinger D, Almazan G, Funnell WRJ, Cuello AC (1997): Quantification of CFOS and glial fibrillary acidic protein in (GFAP) expression following topical application of potassium chloride to the brain surface. Brain Res., 784, 71-81

Huber AM, Koike T, Wada H, Nandapalan V & Fisch U (2001a): Partial fixation of the anterior malleal ligament: diagnosis and consequence on hearing threshold. 24th ARO MidWinter Mtg

Huttenbrink KB.(1995): Die funktion der gehorknochelchenkette und der muskeln des mittelohres. Europ. Arch Oto-Rhino-Laryngology, Suppl. I: 1-52.

Johnson GA et al. (1993): Histology by magnetic-resonance microscopy. Magnetic Resonance Quarterly 9 (1): 1-30.

Khanna SM (1970): A holographic study of tympanic membrane vibrations in cats. University microfilms, Ann Arbor, MI 48104.

Khanna SM, Tonndorf J (1972): Tympanic membrane vibrations in cats studied by time-averaged holography. J. Acoust. Soc. Am. 51: 1904-1920.

Khanna SM, Decraemer WF (1997): Vibrations modes and the middle ear function. Middle ear mechanics in research and Otosurgery. Proceedings of the International Workshop on Middle Ear Mechanics in Research and Otosurgery. Dresden, Germany: Karl-Berndt Huttenbrink, 21-22.

Lim DJ (1968): Tympanic membrane. Electron microscopic observation. Part I. Pars tensa. Acta Otolaryngol. 66: 181-198.

Lippy WH, Schuring AG, Ziv M (1978): Stapedectomy for otosclerosis with malleus fixation. Archives of Otolaryngology. 104(7):388-9.

Manuel J (2002): High-resolution revolution. Environ Health Perspect.;110(5):A238-9.

Margolis RH, Shanks JE (1991): Tympanometry: basic principles and clinical applications. In: Rintelmann WF, ed. Hearing assessment (2nd ed), 179-245.

Margolis RH, Keefe DH (1997): Reflectance tympanometry. The Association for Research in Otolaryngology Annual Mid-Winter Meeting, St. Petersburg Beach, Florida, Abstract #195.

Margolis RH, Schachern PL, Fulton S (1998): Multifrequency tympanometry and histopathology in chinchillas with experimentally produced middle ear pathologies. Acta Oto-Laryngologica; 118(2):216-25.

Mehl AL, Thomson V (1998): Newborn hearing screening: the great omission. Pediatrics; 101(1): E4.

Moon CN Jr, Hahn MJ (1981): Primary malleus fixation; diagnosis and treatment. Laryngoscope. 91 (8):1298-307.

Pederson CB (1994): Revision surgery in otosclerosis–operative findings in 186 patients. Clinical Otolaryngology & Allied Sciences. 19(5):446-50.

Prendergast PJ, Kelly DJ, Rafferty M, et al.(1999): The effect of ventilation tubes on stresses and vibration motion in the tympanic membrane: a finite element analysis. Clin. Otolaryngol.; 24: 542-548.

Rabbitt RD, Holmes MH (1986): A fibrous dynamic continuum model of the tympanic membrane. J Acoust Soc Am, 80, 1716-1728.

Rosowski JJ, Eiber A (1999): Editorial. Audiol Neorootol; 4: 121-122.

Schuknecht HF (1993): Pathology of the ear, 2nd edition. Philadelphia: Lea & Febiger.

Shaw EAG, Stinson MR(1981): Network concepts and energy flow in the human middle ear. Journal of the Acoustical Society of America; 69(S1): 43.

Siah TH & Funnell, WRJ (2001): Modelling the mechanics of the coupling between the incus and stapes in the middle ear. Can. Acoustics 29(3): 38-41.

Siah TH (2002): Finite-element modelling of the mechanics of the coupling between the incus and stapes in the middle ear. Master of Engineering thesis, McGill University, Montreal.

Stakgold I (1968): Boundary value problems of mathematical physics. Vol.II., Macmillan, New York, 332-335.

Subotic R, Mladina R, Risavi R (1998): Congenital bony fixation of the malleus. Acta Otolaryngol; 118(6):833-6.

Tonndorf J, Khanna SM (1972): Tympanic-membrane vibrations in human cadaver ears studied by time-averaged holography. J. Acoust. Soc. Am. 52(4): 1221-1223.

Van Wijhe (2000): A Finite-element model of the middle ear of the moustached bat. Master of Engineering thesis, McGill University, Montreal.

Vlaming, MSMG, Feenstra, L (1986): Studies on the mechanics of the normal human middle ear. Clin. Otolaryngol.; 11: 353-363.

Wada H & Kobayashi T (1990): Dynamical behaviour of middle ear: Theoretical study corresponding to measurement results obtained by a newly developed measuring apparatus. J Acoust Soc Am 87: 237-245.

Wada H, Metoki T, Kobayashi T (1992): Analysis of dynamic behavior of human middle ear using a finite-element method. J Acoust Soc Am.; 96: 3157-3168.

Williams KR, Blayney AW, Rice HJ (1997): Middle ear mechanics as examined by the finite element method. Middle ear mechanics in research and Otosurgery. Proceedings of the International Workshop on Middle Ear Mechanics in Research and Otosurgery. Dresden, Germany: Karl-Berndt Huttenbrink, 67-75.

Wright A. (1997): Anatomy and ultrastructure of the human ear in Kerr A. Scott-Brown's Otolarygology, Basic Sciences, 1-50.

Zhou X, Peck TL, Litchfield JB (1995): Magnetic Resonance Microscopy. Annual reports on NMR spectroscopy, vol. 31, 31-80.

Zienkewicz O, Taylor R (2000): The Finite Element Method, The Basis, vol. 1. Butterworth-Heinemann.

Zwislocki J (1962): Analysis of the middle ear function, Part I input impedance, Journal of the Acoustical Society of America, 34(9): 1514-1523.